The Astronomical Journal, 125:727–741, 2003 February

SPECTRAL ENERGY DISTRIBUTIONS AND AGE ESTIMATES OF 172 GLOBULAR CLUSTERS IN M31

Linhua Jiang,[1,2] Jun Ma,[1] Xu Zhou,[1] Jiansheng Chen,[1] Hong Wu,[1] and Zhaoji Jiang[1]
Received 2002 August 27; accepted 2002 October 31

ABSTRACT

In this paper, we present CCD multicolor photometry for 172 globular clusters (GCs), taken from the Bologna catalog (Battistini et al., published in 1987), in the nearby spiral galaxy M31. The observations were carried out by using the National Astronomical Observatories' 60/90 cm Schmidt telescope in 13 intermediate-band filters, which covered a range of wavelengths from 3800 to 10,000 Å. This provides a multicolor map of M31 in pixels of $1\farcs7 \times 1\farcs7$. By aperture photometry, we obtain the spectral energy distributions for these GCs. Using the relationship between the Beijing-Arizona-Taiwan-Connecticut intermediate-band system used for the observations and the *UBVRI* broadband system, the magnitudes in the *B* and *V* bands are derived. The computed *V* and $B-V$ are in agreement with the values given by Battistini et al. and Barmby et al. (published in 2000). Finally, by comparing the photometry of each GC with theoretical stellar population synthesis models, we estimate ages of the sample GCs for different metallicities. The results show that nearly all our sample GCs have ages of more than 10^9 yr, and most of them are around 10^{10} yr old. In addition, we find that GCs fitted by the metal-poor model are generally older than ones fitted by the metal-rich model.

Key words: galaxies: evolution — galaxies: individual (M31) — globular clusters: general

1. INTRODUCTION

The study of globular clusters (GCs) plays an important role in our understanding of the evolution and structure of galaxies. A single GC is a "packet" of Population II stars with a single age and chemical abundance, so the GCs provide a unique laboratory for exploring dynamics and theoretical evolution of their parent galaxies. GCs are likely to be the oldest known stellar objects, and all large galaxies appear to contain them (Harris 1991). Among the Local Group galaxies, M31 is an ideal target for studying GCs, since it makes up the largest sample of GCs, which is more than all GCs combined in other Local Group members (Battistini et al. 1987; Racine 1991; Harris 1991; Fusi Pecci et al. 1993). It is thus well known that the understanding of M31 GCs is especially important.

M31, a large spiral galaxy, is one of our nearest neighbors, with a distance modulus of 24.47 (Holland 1998; Stanek & Garnavich 1998). Because it is so near and has a very large sample of GCs, M31 is an excellent candidate for GCs studies. The first catalog of 140 clusters in M31 was given by Hubble (1932). From then on, numerous lists of GC candidates were published. A general catalog of almost all the GCs known in the early time was compiled by Vetešník (1962a), who gave a total number of 257 GCs, including most candidates identified by previous works (e.g., Hubble 1932; Seyfert & Nassau 1945; Hiltner 1958; Mayall & Eggen 1953; Kron & Mayall 1960). Later, several major catalogs were compiled by Sargent et al. (1977), Crampton et al. (1985), and Bologna group (Battistini et al. 1980, 1987). Sargent et al. (1977) found or confirmed 355 GCs in their catalog and also rejected 52 candidates obtained by previous surveys. The catalog of Crampton et al. (1985) was a compilation with 509 GC candidates, and the core radii, *V* magnitudes, and intrinsic colors for most candidates were also given or estimated. The most comprehensive catalog of GC candidates may be the Bologna catalog (Battistini et al. 1987). The Bologna group did independent searches for candidates and compiled them with their own Bologna number. The Bologna catalog contains a total of 827 objects, and all the objects were classified into five classes by authors' degree of confidence. Three hundred fifty-three of these candidates were considered to be class A or class B with a high level of confidence, while the others fell into classes C, D, or E. *V* magnitude and $B-V$ color for most candidates were also given in the Bologna catalog.

All GC candidates in these catalogs were carefully selected and usually identified by several steps. However, it is not to say that these samples were clean. They were often contaminated by foreground stars, background galaxies, or other objects (e.g., H II regions). For example, even several class A or B candidates in the Bologna catalog turned out not to be GCs (Barmby et al. 2000). Similarly, these catalogs were not complete, although they may be fairly complete down to $V = 18$ ($M_v \sim -6.5$) (Fusi Pecci et al. 1993). Actually, most candidates in the Bologna catalog also reached down to $V = 18$ (Battistini et al. 1987). As a result, in recent years, many works were searching for new and fainter GCs, especially in the center region of M31 (e.g., Aurière, Coupinot, & Hecquet 1992; Battistini et al. 1993). Additionally, some much fainter GCs were detected by the *Hubble Space Telescope* with high spatial resolution (e.g., Barmby & Huchra 2001; Rich et al. 2001). According to the estimate of Barmby & Huchra (2001), the total number of GCs in M31 is about 460 ± 70.

Anyway, these samples provide a good database for studies of M31 GCs. On the basis of the database, many results were derived and some properties of M31 GCs were well explored, such as luminosity function (e.g., Aurière et al. 1992; Mochejska et al. 1998; Barmby, Huchra, & Brodie 2001), reddening and intrinsic colors (e.g., Vetešník 1962b; Bajaja & Gergely 1977; Iye & Richter 1985; Barmby et al. 2000), metallicities (e.g., van den Bergh 1969; Ashman &

[1] National Astronomical Observatories, Chinese Academy of Sciences, A20 Datun Road, Chaoyang District, Beijing 100012, China; and Chinese Academy of Sciences–Peking University Joint Beijing Astrophysical Center Beijing 100871, China.
[2] Department of Astronomy, Peking University, Beijing, 100871, China.

Bird 1993; Barmby et al. 2000; Perrett et al. 2002), and comparisons with the Galactic GCs and M33 GCs (e.g., Hiltner 1960; Frogel, Persson, & Cohen 1980; Reed, Harris, & Harris 1992; Mochejska et al. 1998).

Although there are already much observation information and theoretical results in previous studies, for full physical information about the GCs, it is of great value to obtain multiband photometry, which can provide their accurate spectral energy distributions (SEDs). In addition, we can estimate GC ages by comparing their intrinsic SEDs with ones of theoretical stellar population synthesis models. The GC ages are important, they can provide us with information on the early formative stages of the parent galaxy and can be used to provide a lower limit to the age of the parent galaxy. The distribution of GC ages can be used especially to understand the conditions for their formation. For example, Barmby & Huchra (2000) presented that conditions for cluster formation must have existed for a substantial fraction of the parent galaxy's lifetime by comparing three sets of population synthesis models with integrated colors of M31 and Galactic GCs in the set of *UBVRIJHK*. However, ages of most individual GCs in M31 remain undetermined, although they have been derived for a few. For example, Jablonka, Alloin, & Bica (1992) presented spectrophotometric data for seven GCs and derived their reddening, metallicities, and ages. According to the calculation of Borges et al. (1995), de Freitas Pacheco (1997) reported a sample of 12 GCs and obtained the mean age of the sample.

In this paper, we present CCD spectrophotometry of a set of GCs in M31 using images obtained with the Beijing-Arizona-Taiwan-Connecticut (BATC) Multicolor Sky Survey Telescope designed to obtain SED information for galaxies (Fan et al. 1996). The BATC system uses the 60/90 cm Schmidt telescope with 15 intermediate bandwidth filters. In this study, we use 13 of these filters, from 3800 to 10,000 Å, with images covering the most visible extent of M31 and present the SEDs of 172 GCs selected from the Bologna catalog (Battistini et al. 1987). Using previously derived relationships between the BATC intermediate-band system, we go on to compute the B and V magnitudes for these objects. The computed V magnitudes and $B-V$ colors are in good agreement with the values given by Battistini et al. (1987) and Barmby et al. (2000). We also plot histograms of the V-band magnitudes and of $B-V$ colors, as well as plotting the corresponding color-magnitude diagram for our sample GCs. Since reddening of GCs in M31 was determined by several authors (e.g., Vetešník 1962b; Crampton et al. 1985; Barmby et al. 2000), we can infer the intrinsic colors for each individual GC. Finally, using theoretical stellar population synthesis models, we estimate ages of our sample GCs. The results show that most objects are as old as about 10^{10} yr, and GCs fitted by the metal-poor model are generally older than ones fitted by the metal-rich model.

This paper will take the following form: § 2 presents our sample GCs and details of observations and data reduction. We also obtain SEDs and give comparisons of GC photometry between the BATC system and previous measurements in this section. In § 3, we briefly describe the stellar population synthesis models of simple stellar populations from the Galaxy Isochrone Synthesis Spectra Evolution Library (hereafter GSSPs; G. Bruzual & S. Charlot 1996, unpublished). We present how we deredden the sample GCs in § 4. In § 5, ages for the GCs are estimated for different values of metallicity. Finally, we give a summary in § 6.

2. SAMPLE OF GCs, OBSERVATIONS, AND DATA REDUCTION

2.1. *Selection of Sample*

The GC candidates in each catalog were carefully selected and identified by different ways or several steps; however, the catalogs of GCs were often contaminated by stars, background galaxies, or other objects such as H II regions. The basic idea of the identification of a new GC candidate is the fact that the point-spread function of a GC has a larger FWHM than a star (Mochejska et al. 1998). In general, observers discover a new GC first using visual inspection, i.e., they distinguish cluster images from stars or spurious nonstellar objects by image morphology (Battistini et al. 1987). For example, objects that appear asymmetrical or exhibit structure are usually not GCs, thus most open clusters and background galaxies that are asymmetrical or display structure are easily eliminated (Crampton et al. 1985). Sometimes identifying a new GC in the center region or in the halo of M31 needs other means. Due to the strong background gradient, the identification of candidates in the center region by image morphology may be less efficient. Aurière et al. (1992) used another powerful method, the wavelet analysis, to reduce the image. For the candidates in the M31 halo, there are also several other ways to define a clean sample (see Reed, Harris, & Harris 1992 for a detail).

The sample of GCs chosen in this paper is from the Bologna catalog by Battistini et al. (1987). As has been mentioned, the Bologna catalog with a total of 827 GC candidates, is the most comprehensive catalog of M31 GCs. All the candidates were classified into five classes by authors' degree of confidence. Three hundred fifty-three of all the candidates were considered to be class A (254 objects) and class B (99 objects) with a very high level of confidence, 152 candidates were listed in class C, and the others fell into classes D and E. Our selection of the sample is as follows. First, we take all candidates of classes A and B (i.e., Table IV of Bologna catalog) as our original sample. We find that only 223 objects are in our CCD field. Then we note that clusters 7, 55, 132, and 147 are virtually stars, not true GCs (Barmby et al. 2000), so they are not included in our sample. As a result, there are 219 class A or B GCs of the Bologna catalog in our CCD field. In addition, 47 of the 219 GCs, which are saturated in some filters, are also excluded from our sample. At last, 172 GCs are included here. Since our sample candidates in the Bologna catalog are classified into classes A and B by the authors' high level of confidence and cross-checked by others (e.g., Barmby et al. 2000), we consider that these objects are GCs, and we do not confirm them again. In addition, we should emphasize that the numbering system of the Bologna catalog is adopted in this paper.

2.2. *Observations and Data Reduction*

The large field multicolor observations of M31 were obtained in the BATC photometric system, in which a 60/90 cm f/3 Schmidt telescope is used. This telescope is located at Xinglong Station of National Astronomical Observatories. A Ford Aerospace 2048 × 2048 CCD camera with 15 μm pixel size is mounted at the Schmidt focus, giving a CCD field of view of $58' \times 58'$ with a pixel size of $1''.7$.

TABLE 1
PARAMETERS OF THE BATC FILTERS AND STATISTICS OF OBSERVATIONS

No. (1)	Name (2)	CW[a] (Å) (3)	Exp.[b] (4)	N. Img.[c] (5)	rms[d] (6)
1.....	BATC03	4210	01:00	03	0.015
2.....	BATC04	4546	05:30	17	0.009
3.....	BATC05	4872	03:30	11	0.015
4.....	BATC06	5250	02:20	12	0.006
5.....	BATC07	5785	02:15	07	0.003
6.....	BATC08	6075	01:40	05	0.003
7.....	BATC09	6710	00:45	03	0.003
8.....	BATC10	7010	03:00	12	0.008
9.....	BATC11	7530	02:00	06	0.004
10.....	BATC12	8000	04:00	12	0.003
11.....	BATC13	8510	01:30	05	0.004
12.....	BATC14	9170	05:50	18	0.003
13.....	BATC15	9720	04:00	12	0.009

[a] Central wavelength for each BATC filter.
[b] Exposure time is in hours and minutes.
[c] Image numbers for each BATC filter.
[d] Zero-point error, in magnitude, for each filter as obtained from the standard stars.

The multiband BATC filter system comprises 15 intermediate-band filters, covering the full optical wavelength range from 3000 to 10,000 Å. The filters were designed specifically to avoid contamination from the brightest and most variable night-sky emission lines. Details of the Schmidt telescope, the CCD camera, the data acquisition system, and the definition of the BATC filter passbands can be found in previous publications (Fan et al. 1996; Zheng et al. 1999). The observations of M31 were carried out from 1995 September 15 through 1999 December 16, with a total exposure time of about 37 hr 20 minutes, while the CCD images were accumulated in 13 of the BATC filters. The dome flats were obtained using a diffuser plate in front of the Schmidt corrector plate. For flux calibration, the Oke-Gunn primary standard stars HD 19445, HD 84937, BD $+26^{\circ}2606$, and BD $+17^{\circ}4708$ were observed under photometric conditions (see Yan et al. 2000 and Zhou et al. 2001 for details). The parameters of the filters, and the basic statistics of the observations are given in Table 1.

Using standard procedures, the data were reduced by automatic reduction software: PIPELINE I, which includes bias subtraction and flat fielding of the CCD images. This software was developed for the BATC multicolor sky survey (see Ma et al. 2001, 2002a for details). The absolute flux of images was calibrated using observations of standard stars. Fluxes, as observed through the BATC filters for the Oke-Gunn stars, were derived by convolving the SEDs of these stars with the measured BATC filter transmission functions (Fan et al. 1996). In Table 1, column (6) gives the zero-point errors in magnitude for the standard stars through each filter. The formal errors obtained for these stars in the 13 BATC filters used are $\lesssim 0.02$ mag, which implies that we can define photometrically the BATC system to an accuracy of better than 0.02 mag.

2.3. *Integrated Photometry*

To obtain the magnitude of a given GC, the PHOT routine in DAOPHOT (Stetson 1987, 1990) is used. For avoiding contamination from nearby objects, we adopt a small aperture diameter of 10.″2, which corresponds to a diameter of 6 pixels in Ford CCDs. Aperture corrections are computed using isolated stars. Finally, we obtained the SEDs in 13 BATC filters for 172 GCs, which are listed in Table 2. The table contains the following information: Column (1) is the cluster number taken from the Bologna catalog (Battistini et al. 1987). Columns (2)–14 present the magnitudes in the selected BATC bands, and on a second row for each GC in these columns, we give the magnitude uncertainty for each band. The uncertainties are given by DAOPHOT.

2.4. *Magnitudes in the B and V Bands, and B−V Colors*

Using Landolt standards and the catalogs of Landolt (1983, 1992) and of Galadí-Enríquez, Trullols, & Jordi (2000), Zhou et al. (2002) derived the relationships between the BATC intermediate-band system and the *UBVRI* broadband system. These relationships are given in equations (1) and (2) as

$$m_B = m_{04} + (0.2218 \pm 0.033)(m_{03} - m_{05}) + 0.0741 \pm 0.033 , \quad (1)$$

$$m_V = m_{07} + (0.3233 \pm 0.019)(m_{06} - m_{08}) + 0.0590 \pm 0.010 . \quad (2)$$

Using equations (1) and (2), we transformed the magnitudes of the 172 GCs in the BATC03, BATC04, and BATC05 bands into *B*-band magnitudes and also derived *V*-band magnitudes from those in BATC06, BATC07, and BATC08.

Histograms of the computed V magnitudes and $B-V$ colors and color-magnitude diagram, V against $B-V$, are shown in Figure 1. The figure is in good agreement with the corresponding plots of classes A and B GCs given by Battistini et al. (1987). From the left panel of Figure 1, we can see that most of our sample GCs are brighter than $V = 18$. This relates to the original catalog, because V magnitudes of most class A and B GCs in Bologna catalog are brighter than 18 mag. The right panel of Figure 1 shows that $B-V$ colors of most GCs are redder than 0.6, which is reasonable. Actually, the GCs are generally the objects with $B-V > 0.6$ (Crampton et al. 1985) or $B-V > 0.55$ (Barmby et al. 2000). Iye & Richter (1985) even considered $B-V < 0.6$ 0.6 as one of their criteria of rejecting GC candidates.

We also present the comparisons of the BATC photometry with previously published measurements (Battistini et al. 1987; Barmby et al. 2000) in Figures 2 and 3. These figures do not present all GCs of our sample, since V magnitudes and $B-V$ colors of some GCs were not given by Battistini et al. (1987) and Barmby et al. (2000). Figure 2 plots the comparison for 157 objects, while Figure 3 plots it for 141 objects. From these figures, it can be seen that there are good agreements between the BATC photometry and the other two photometric measurements. In Figure 2, the differences of V magnitudes for several objects are abnormally big, such as clusters 118, 127, 131, 138, and 186. The reason may be that clusters 118, 127, 131, and 138 lie in the center region of the parent galaxy, so we cannot subtract the background very well. However, the BATC V magnitude of cluster 186 is in good agreement with the value presented by Barmby et al. (2000). The mean differences of V and $B-V$ between the BATC photometry and Battistini et al. (the

TABLE 2

SEDs OF 172 GCs IN M31

No. (1)	03 (2)	04 (3)	05 (4)	06 (5)	07 (6)	08 (7)	09 (8)	10 (9)	11 (10)	12 (11)	13 (12)	14 (13)	15 (14)
326.....	16.18	16.16	16.01	16.00	15.78	15.81	15.77	15.69	15.64	15.51	15.47	15.43	15.44
	0.175	0.173	0.185	0.188	0.186	0.197	0.198	0.202	0.206	0.211	0.220	0.212	0.219
328.....	17.43	17.14	16.92	16.84	16.50	16.49	16.42	16.31	16.21	16.03	15.96	15.96	16.01
	0.106	0.162	0.163	0.162	0.153	0.159	0.159	0.158	0.165	0.159	0.163	0.161	0.177
332.....	19.27	18.90	18.74	18.91	18.59	18.58	18.51	18.68	18.22	17.96	17.67	18.16	17.67
	0.250	0.225	0.262	0.321	0.337	0.356	0.375	0.488	0.369	0.340	0.301	0.463	0.311
333.....	19.35	18.90	18.74	18.48	18.13	18.11	17.86	17.82	17.52	17.50	17.49	17.10	17.24
	0.300	0.245	0.282	0.238	0.239	0.250	0.221	0.241	0.211	0.240	0.279	0.185	0.221
9.....	17.82	17.38	17.12	17.04	16.69	16.65	16.55	16.50	16.38	16.24	16.35	16.24	16.25
	0.028	0.022	0.020	0.021	0.021	0.021	0.022	0.025	0.028	0.025	0.042	0.028	0.040
11.....	17.61	17.17	16.87	16.76	16.41	16.36	16.24	16.16	16.04	15.93	15.97	15.90	15.90
	0.038	0.031	0.031	0.030	0.031	0.030	0.030	0.032	0.035	0.036	0.042	0.041	0.043
14.....	20.15	19.23	18.51	18.14	17.80	17.64	17.33	17.28	17.19	17.07	16.80	16.70	16.52
	0.103	0.045	0.027	0.024	0.024	0.019	0.022	0.013	0.018	0.008	0.038	0.009	0.038
15.....	19.20	18.59	18.25	17.93	17.50	17.36	17.02	16.83	16.60	16.42	16.45	16.05	16.01
	0.108	0.063	0.059	0.046	0.039	0.036	0.027	0.026	0.023	0.020	0.036	0.019	0.029
17.....	17.16	16.72	16.36	16.10	15.69	15.59	15.32	15.18	15.04	14.90	14.86	14.66	14.59
	0.012	0.006	0.005	0.005	0.004	0.004	0.004	0.004	0.004	0.003	0.007	0.004	0.008
21.....	18.73	18.25	17.93	17.69	17.31	17.21	16.92	16.76	16.59	16.43	16.44	16.13	16.10
	0.048	0.037	0.031	0.031	0.030	0.027	0.025	0.023	0.024	0.021	0.030	0.023	0.034
23.....	15.49	14.98	14.63	14.35	13.95	13.85	13.58	13.44	13.29	13.17	13.11	12.90	12.85
	0.003	0.002	0.002	0.002	0.002	0.001	0.001	0.001	0.001	0.001	0.002	0.002	0.002
25.....	17.69	17.36	17.10	16.87	16.56	16.49	16.24	16.16	16.09	16.02	16.01	15.86	15.87
	0.015	0.012	0.011	0.012	0.012	0.010	0.012	0.014	0.017	0.014	0.025	0.024	0.031
27.....	16.41	16.12	15.90	15.73	15.45	15.39	15.19	15.09	15.05	15.00	14.99	14.83	14.83
	0.007	0.007	0.006	0.006	0.006	0.006	0.005	0.005	0.005	0.005	0.008	0.007	0.010
28.....	17.63	17.37	17.12	16.97	16.72	16.67	16.43	16.33	16.27	16.21	16.20	16.01	16.00
	0.013	0.012	0.011	0.011	0.012	0.010	0.012	0.013	0.017	0.014	0.026	0.024	0.032
29.....	17.88	17.37	17.06	16.86	16.52	16.43	16.18	16.05	15.87	15.81	15.79	15.49	15.46
	0.018	0.014	0.012	0.012	0.011	0.009	0.010	0.010	0.011	0.011	0.015	0.014	0.018
30.....	19.28	18.55	18.20	17.80	17.28	17.13	16.74	16.54	16.32	16.19	16.12	15.77	15.70
	0.116	0.075	0.072	0.048	0.037	0.028	0.029	0.020	0.020	0.018	0.030	0.018	0.024
31.....	19.19	18.56	18.23	17.93	17.51	17.36	17.14	16.99	16.88	16.77	16.62	16.53	16.69
	0.071	0.056	0.049	0.040	0.036	0.031	0.027	0.027	0.029	0.025	0.039	0.034	0.050
32.....	19.07	18.41	17.99	17.73	17.32	17.23	16.92	16.78	16.63	16.47	16.41	16.16	16.13
	0.049	0.031	0.027	0.024	0.025	0.022	0.020	0.018	0.019	0.018	0.025	0.019	0.028
33.....	19.03	18.80	18.45	18.18	17.89	17.70	17.52	17.35	17.45	17.35	17.29	17.16	17.05
	0.071	0.074	0.067	0.056	0.056	0.045	0.044	0.043	0.052	0.050	0.064	0.065	0.075
34.....	16.46	16.03	15.77	15.59	15.28	15.23	14.98	14.87	14.76	14.71	14.74	14.49	14.50
	0.006	0.004	0.003	0.003	0.004	0.004	0.004	0.004	0.004	0.004	0.008	0.005	0.007
36.....	18.38	17.96	17.64	17.45	17.09	16.97	16.79	16.70	16.53	16.45	16.34	16.20	16.20
	0.022	0.014	0.010	0.011	0.013	0.010	0.012	0.012	0.016	0.012	0.030	0.021	0.030
37.....	19.28	18.47	17.81	17.23	16.40	16.14	15.54	15.25	14.89	14.61	14.32	13.95	13.78
	0.061	0.032	0.021	0.016	0.012	0.009	0.007	0.006	0.006	0.004	0.007	0.004	0.005
38.....	17.35	17.04	16.74	16.56	16.22	16.13	15.94	15.82	15.74	15.65	15.56	15.43	15.38
	0.014	0.011	0.009	0.009	0.009	0.009	0.009	0.009	0.010	0.011	0.017	0.014	0.018
39.....	17.44	16.91	16.51	16.23	15.75	15.63	15.34	15.19	15.00	14.88	14.71	14.54	14.49
	0.016	0.010	0.009	0.008	0.007	0.006	0.005	0.005	0.006	0.005	0.009	0.006	0.008
41.....	18.82	18.26	17.96	17.88	17.43	17.35	17.19	17.05	16.95	16.86	16.73	16.73	16.66
	0.131	0.106	0.107	0.108	0.098	0.097	0.094	0.092	0.097	0.100	0.111	0.101	0.101
42.....	18.03	17.44	16.93	16.47	15.89	15.71	15.32	15.13	14.94	14.76	14.63	14.40	14.34
	0.071	0.062	0.056	0.044	0.039	0.036	0.030	0.028	0.027	0.026	0.027	0.022	0.021
44.....	17.92	17.44	17.07	16.85	16.45	16.34	16.12	15.97	15.84	15.72	15.61	15.45	15.44
	0.022	0.013	0.011	0.010	0.010	0.008	0.009	0.009	0.010	0.008	0.016	0.012	0.017
48.....	17.60	17.14	16.82	16.63	16.28	16.21	15.98	15.85	15.72	15.61	15.55	15.32	15.31
	0.023	0.021	0.019	0.018	0.019	0.018	0.018	0.019	0.020	0.021	0.025	0.024	0.026
51.....	17.44	16.93	16.54	16.29	15.87	15.77	15.52	15.38	15.22	15.09	14.99	14.82	14.79
	0.011	0.007	0.006	0.005	0.005	0.004	0.004	0.004	0.005	0.004	0.007	0.007	0.009
53.....	18.91	18.47	18.18	18.11	17.80	17.78	17.69	17.63	17.58	17.49	17.50	17.39	17.28
	0.053	0.045	0.038	0.042	0.045	0.042	0.048	0.051	0.056	0.065	0.078	0.086	0.090
54.....	19.07	18.68	18.34	18.18	17.84	17.84	17.59	17.43	17.20	17.17	17.15	16.74	16.65
	0.066	0.065	0.053	0.055	0.052	0.049	0.051	0.051	0.054	0.054	0.060	0.058	0.064
56.....	18.38	17.84	17.55	17.38	17.01	16.97	16.69	16.57	16.37	16.32	16.33	16.00	15.89
	0.032	0.024	0.018	0.018	0.020	0.018	0.017	0.019	0.018	0.020	0.026	0.022	0.026

TABLE 2—*Continued*

No. (1)	03 (2)	04 (3)	05 (4)	06 (5)	07 (6)	08 (7)	09 (8)	10 (9)	11 (10)	12 (11)	13 (12)	14 (13)	15 (14)
57.....	18.32	17.99	17.81	17.69	17.45	17.44	17.20	17.16	17.20	17.14	17.14	17.07	17.16
	0.041	0.034	0.033	0.031	0.033	0.032	0.031	0.033	0.045	0.046	0.064	0.064	0.094
59.....	18.16	17.78	17.40	17.18	16.80	16.70	16.47	16.34	16.25	16.13	16.01	15.91	15.88
	0.149	0.151	0.142	0.122	0.115	0.108	0.094	0.093	0.098	0.093	0.097	0.090	0.090
60.....	17.36	17.12	16.90	16.72	16.51	16.47	16.32	16.23	16.17	16.14	16.02	15.93	15.97
	0.015	0.016	0.016	0.017	0.018	0.018	0.020	0.020	0.022	0.021	0.028	0.029	0.036
61.....	17.93	17.40	17.02	16.81	16.31	16.23	16.11	15.82	15.59	15.49	15.41	15.17	15.13
	0.021	0.016	0.013	0.012	0.010	0.009	0.010	0.008	0.008	0.007	0.013	0.010	0.013
63.....	17.06	16.51	16.08	15.85	15.36	15.26	14.99	14.84	14.64	14.55	14.46	14.19	14.16
	0.011	0.007	0.005	0.005	0.004	0.004	0.004	0.004	0.004	0.004	0.006	0.004	0.006
64.....	17.01	16.72	16.45	16.29	16.05	15.99	15.82	15.73	15.62	15.56	15.49	15.39	15.44
	0.019	0.021	0.021	0.020	0.022	0.021	0.021	0.023	0.025	0.028	0.031	0.031	0.036
67.....	17.90	17.60	17.37	17.24	17.02	16.99	16.81	16.73	16.69	16.69	16.51	16.59	16.71
	0.020	0.021	0.021	0.022	0.026	0.026	0.032	0.031	0.042	0.043	0.052	0.057	0.078
68.....	17.70	17.11	16.76	16.49	16.07	15.96	15.64	15.51	15.34	15.29	15.17	14.91	14.90
	0.020	0.014	0.010	0.009	0.008	0.007	0.007	0.006	0.007	0.006	0.011	0.007	0.012
69.....	18.54	18.42	18.18	18.18	18.02	18.02	17.86	17.88	17.90	17.87	17.82	17.88	17.73
	0.034	0.034	0.032	0.037	0.048	0.044	0.051	0.053	0.065	0.059	0.134	0.106	0.138
70.....	17.45	17.21	16.98	16.83	16.59	16.55	16.39	16.32	16.28	16.21	16.18	16.07	16.05
	0.017	0.017	0.016	0.017	0.018	0.015	0.020	0.020	0.023	0.023	0.033	0.033	0.045
71.....	19.49	18.87	18.49	18.19	17.82	17.65	17.36	17.16	17.01	16.80	16.87	16.82	16.98
	0.160	0.130	0.122	0.113	0.118	0.107	0.108	0.097	0.104	0.100	0.134	0.144	0.184
72.....	18.19	17.99	17.66	17.39	16.81	16.61	16.40	16.13	15.88	15.66	15.38	15.35	15.22
	0.033	0.040	0.042	0.036	0.032	0.026	0.027	0.025	0.025	0.022	0.026	0.026	0.023
73.....	17.00	16.51	16.23	16.07	15.76	15.72	15.51	15.40	15.27	15.26	15.16	15.00	15.00
	0.018	0.013	0.013	0.011	0.012	0.010	0.010	0.010	0.012	0.011	0.019	0.013	0.018
75.....	18.29	17.88	17.56	17.39	17.03	16.95	16.76	16.65	16.55	16.45	16.29	16.24	16.27
	0.034	0.031	0.029	0.028	0.030	0.029	0.032	0.032	0.037	0.039	0.045	0.050	0.058
76.....	17.63	17.30	17.01	16.82	16.57	16.51	16.31	16.20	16.15	16.10	16.03	15.91	15.98
	0.019	0.016	0.016	0.016	0.017	0.016	0.019	0.019	0.024	0.024	0.035	0.032	0.042
77.....	19.12	18.36	17.94	17.56	17.19	17.04	16.77	16.61	16.45	16.34	16.29	16.08	16.05
	0.144	0.101	0.087	0.065	0.059	0.047	0.041	0.037	0.038	0.034	0.046	0.039	0.047
78.....	20.01	18.88	18.39	17.99	17.37	17.28	16.86	16.69	16.46	16.28	16.09	15.91	15.87
	0.521	0.295	0.262	0.214	0.177	0.178	0.146	0.141	0.133	0.129	0.121	0.113	0.110
79.....	19.56	18.75	18.27	17.91	17.54	17.33	17.04	16.89	16.71	16.52	16.35	16.06	16.03
	0.091	0.054	0.039	0.032	0.030	0.025	0.023	0.023	0.021	0.020	0.025	0.021	0.030
80.....	19.21	18.71	18.15	17.73	17.18	16.97	16.66	16.49	16.32	16.15	15.98	15.80	15.78
	0.225	0.212	0.177	0.132	0.111	0.097	0.083	0.079	0.079	0.078	0.083	0.069	0.071
82.....	17.38	16.70	16.19	15.75	15.19	15.03	14.60	14.41	14.21	14.07	13.92	13.68	13.64
	0.020	0.016	0.012	0.009	0.006	0.006	0.004	0.004	0.004	0.004	0.005	0.004	0.005
84.....	19.86	19.18	18.81	18.35	17.85	17.72	17.39	17.23	16.93	16.77	16.64	16.52	16.48
	0.277	0.204	0.206	0.157	0.145	0.144	0.124	0.124	0.113	0.125	0.120	0.122	0.126
86.....	15.73	15.47	15.19	15.08	14.84	14.81	14.66	14.57	14.54	14.47	14.37	14.34	14.36
	0.028	0.030	0.031	0.029	0.032	0.031	0.030	0.030	0.034	0.037	0.038	0.036	0.039
88.....	16.64	16.26	15.86	15.60	15.16	15.05	14.80	14.66	14.52	14.36	14.26	14.09	14.06
	0.008	0.006	0.004	0.004	0.004	0.003	0.003	0.003	0.003	0.003	0.005	0.004	0.005
90.....	19.19	18.53	18.33	18.25	18.03	18.05	17.81	17.80	17.70	17.87	17.83	17.44	17.51
	0.133	0.091	0.103	0.106	0.102	0.106	0.102	0.113	0.126	0.169	0.193	0.147	0.183
91.....	17.82	17.61	17.49	17.47	17.27	17.28	17.25	17.18	17.21	17.15	17.04	17.06	17.23
	0.039	0.041	0.049	0.053	0.057	0.061	0.069	0.073	0.090	0.094	0.111	0.129	0.166
92.....	17.76	17.44	17.17	17.01	16.74	16.68	16.51	16.40	16.37	16.29	16.22	16.14	16.14
	0.034	0.035	0.034	0.035	0.038	0.037	0.039	0.040	0.048	0.050	0.057	0.065	0.072
93.....	17.89	17.51	17.12	16.92	16.59	16.51	16.30	16.14	15.96	15.79	15.65	15.52	15.50
	0.047	0.045	0.042	0.039	0.040	0.039	0.038	0.036	0.034	0.034	0.035	0.035	0.038
94.....	16.62	16.14	15.86	15.69	15.37	15.31	15.06	14.95	14.83	14.79	14.77	14.52	14.51
	0.008	0.005	0.005	0.004	0.004	0.003	0.004	0.004	0.004	0.004	0.006	0.005	0.008
96.....	17.78	17.19	16.78	16.59	16.15	16.00	15.77	15.62	15.44	15.30	15.11	15.04	15.00
	0.126	0.111	0.108	0.101	0.094	0.088	0.082	0.080	0.079	0.081	0.077	0.074	0.072
97.....	18.04	17.60	17.19	16.98	16.56	16.47	16.28	16.14	16.02	15.93	15.78	15.67	15.63
	0.027	0.025	0.022	0.021	0.020	0.019	0.020	0.019	0.021	0.021	0.025	0.025	0.030
98.....	17.17	16.76	16.49	16.32	16.03	15.97	15.76	15.68	15.61	15.56	15.48	15.35	15.40
	0.011	0.007	0.007	0.007	0.007	0.006	0.007	0.007	0.008	0.007	0.014	0.011	0.017
99.....	17.57	17.24	16.93	16.83	16.53	16.50	16.39	16.23	16.16	16.09	15.97	15.81	15.82
	0.047	0.047	0.054	0.049	0.055	0.056	0.058	0.058	0.066	0.071	0.078	0.074	0.083

TABLE 2—*Continued*

No. (1)	03 (2)	04 (3)	05 (4)	06 (5)	07 (6)	08 (7)	09 (8)	10 (9)	11 (10)	12 (11)	13 (12)	14 (13)	15 (14)
101.....	17.73	17.38	17.11	16.97	16.70	16.65	16.44	16.36	16.19	16.09	16.00	15.85	15.81
	0.036	0.038	0.039	0.040	0.044	0.044	0.040	0.044	0.045	0.050	0.055	0.049	0.056
103.....	16.36	15.81	15.44	15.27	14.93	14.84	14.61	14.48	14.31	14.23	14.07	13.93	13.92
	0.077	0.068	0.066	0.061	0.061	0.060	0.054	0.054	0.054	0.059	0.058	0.052	0.054
102.....	17.21	16.94	16.72	16.66	16.41	16.38	16.33	16.24	16.22	16.13	16.15	16.08	16.07
	0.010	0.008	0.007	0.008	0.010	0.009	0.011	0.012	0.015	0.015	0.026	0.023	0.032
104.....	17.65	17.32	17.10	17.02	16.75	16.68	16.58	16.55	16.51	16.38	16.11	16.69	16.82
	0.262	0.279	0.322	0.321	0.362	0.363	0.373	0.407	0.475	0.485	0.433	0.769	0.911
105.....	18.19	17.74	17.44	17.26	16.94	16.86	16.70	16.58	16.43	16.36	16.24	16.09	16.07
	0.023	0.014	0.012	0.012	0.014	0.013	0.014	0.015	0.017	0.016	0.027	0.020	0.028
106.....	17.00	16.56	16.18	16.02	15.68	15.63	15.41	15.31	15.19	15.11	14.99	14.94	14.96
	0.056	0.056	0.055	0.053	0.056	0.058	0.055	0.057	0.061	0.069	0.071	0.073	0.081
108.....	18.34	17.96	17.68	17.51	17.23	17.13	16.93	16.80	16.67	16.65	16.50	16.32	16.27
	0.060	0.059	0.062	0.062	0.072	0.069	0.071	0.071	0.079	0.095	0.089	0.080	0.084
107.....	16.77	16.38	16.04	15.87	15.55	15.44	15.24	15.18	15.08	14.99	14.82	14.78	14.79
	0.038	0.041	0.042	0.039	0.041	0.041	0.039	0.042	0.046	0.054	0.052	0.051	0.054
109.....	17.46	17.00	16.66	16.51	16.15	16.05	15.88	15.74	15.55	15.50	15.30	15.14	15.09
	0.046	0.049	0.044	0.046	0.052	0.049	0.049	0.050	0.053	0.057	0.055	0.053	0.056
111.....	17.51	17.23	17.00	16.84	16.60	16.57	16.36	16.28	16.25	16.22	16.15	16.07	16.06
	0.017	0.014	0.012	0.011	0.013	0.012	0.012	0.013	0.016	0.014	0.026	0.024	0.031
110.....	16.08	15.69	15.41	15.25	14.97	14.92	14.71	14.60	14.50	14.44	14.36	14.23	14.23
	0.005	0.004	0.003	0.004	0.004	0.003	0.004	0.004	0.004	0.004	0.007	0.006	0.008
112.....	17.45	16.84	16.47	16.34	15.98	15.87	15.63	15.49	15.27	15.21	15.02	14.90	14.88
	0.291	0.241	0.236	0.227	0.230	0.223	0.201	0.200	0.192	0.217	0.209	0.192	0.196
114.....	17.40	17.16	16.90	16.75	16.54	16.48	16.35	16.23	16.15	16.06	15.90	15.65	15.59
	0.113	0.136	0.152	0.147	0.175	0.177	0.188	0.188	0.213	0.239	0.235	0.204	0.203
117.....	16.98	16.70	16.50	16.35	16.08	16.10	15.87	15.84	15.82	15.74	15.72	15.59	15.65
	0.012	0.011	0.011	0.014	0.014	0.013	0.012	0.011	0.014	0.017	0.021	0.020	0.033
115.....	16.91	16.34	15.95	15.84	15.45	15.36	15.17	15.03	14.86	14.77	14.60	14.47	14.40
	0.150	0.132	0.131	0.131	0.133	0.132	0.127	0.130	0.133	0.143	0.145	0.131	0.130
116.....	18.45	17.81	17.36	17.00	16.44	16.28	15.95	15.77	15.53	15.36	15.18	14.95	14.86
	0.026	0.016	0.013	0.011	0.011	0.008	0.007	0.007	0.008	0.007	0.011	0.008	0.010
118.....	16.75	16.39	16.02	15.92	15.58	15.53	15.37	15.31	15.18	15.08	14.98	14.89	14.95
	0.224	0.240	0.244	0.248	0.263	0.272	0.274	0.296	0.316	0.334	0.363	0.348	0.390
122.....	19.53	18.81	18.32	17.96	17.35	17.16	16.83	16.64	16.42	16.22	16.12	15.82	15.72
	0.056	0.038	0.025	0.022	0.019	0.015	0.014	0.013	0.014	0.013	0.021	0.016	0.020
123.....	18.29	17.85	17.50	17.36	17.09	17.02	16.79	16.69	16.59	16.51	16.37	16.34	16.33
	0.119	0.123	0.121	0.119	0.135	0.133	0.126	0.131	0.144	0.164	0.169	0.167	0.178
125.....	17.18	16.91	16.68	16.54	16.32	16.30	16.13	16.03	16.01	15.98	15.86	15.81	15.89
	0.011	0.012	0.013	0.013	0.015	0.015	0.017	0.018	0.022	0.022	0.030	0.025	0.036
126.....	17.63	17.27	17.04	16.82	16.52	16.48	16.33	16.22	16.07	16.03	15.80	15.93	15.83
	0.194	0.209	0.239	0.215	0.238	0.244	0.249	0.258	0.271	0.312	0.292	0.348	0.329
127.....	15.08	14.65	14.31	14.17	13.84	13.77	12.33	13.48	13.36	13.27	13.11	13.09	13.07
	0.092	0.093	0.096	0.093	0.100	0.101	0.031	0.102	0.111	0.118	0.122	0.125	0.129
353.....	15.43	14.87	14.45	14.31	13.85	13.73	13.39	13.40	13.11	12.95	12.70	12.68	12.60
	0.380	0.351	0.341	0.333	0.320	0.310	0.148	0.308	0.287	0.281	0.278	0.284	0.278
128.....	17.85	17.38	17.03	16.91	16.68	16.57	16.45	16.26	16.12	16.01	15.83	15.73	15.77
	0.094	0.089	0.086	0.087	0.098	0.095	0.098	0.095	0.101	0.112	0.103	0.100	0.110
130.....	18.03	17.59	17.17	16.96	16.58	16.44	16.24	16.09	16.00	15.85	15.68	15.62	15.62
	0.041	0.037	0.033	0.028	0.026	0.023	0.021	0.021	0.021	0.020	0.023	0.022	0.026
131.....	15.84	15.38	15.03	14.90	14.55	14.47	14.33	14.22	14.08	13.93	13.75	13.74	13.73
	0.155	0.156	0.160	0.157	0.166	0.165	0.168	0.173	0.183	0.187	0.190	0.197	0.204
133.....	17.47	17.47	17.33	17.30	17.23	17.21	17.11	16.97	16.74	16.71	16.60	16.57	16.59
	0.100	0.123	0.141	0.142	0.167	0.169	0.165	0.159	0.138	0.152	0.166	0.153	0.163
134.....	17.14	16.71	16.49	16.29	15.98	15.90	15.74	15.60	15.51	15.42	15.23	15.18	15.32
	0.187	0.190	0.219	0.200	0.220	0.219	0.221	0.221	0.247	0.270	0.265	0.261	0.310
135.....	16.95	16.60	16.26	16.08	15.73	15.64	15.46	15.35	15.24	15.15	15.05	14.94	14.91
	0.008	0.007	0.005	0.006	0.006	0.005	0.006	0.006	0.007	0.007	0.010	0.009	0.012
136.....	17.20	16.83	16.51	16.44	16.27	16.24	16.11	16.06	16.04	15.92	15.69	15.76	15.73
	0.102	0.108	0.113	0.119	0.147	0.153	0.156	0.173	0.208	0.221	0.206	0.235	0.240
137.....	19.22	18.68	18.25	17.93	17.46	17.33	17.05	16.87	16.72	16.56	16.44	16.21	16.15
	0.063	0.049	0.043	0.033	0.032	0.030	0.024	0.024	0.026	0.026	0.036	0.025	0.033
138.....	16.93	16.46	16.11	16.00	15.68	15.62	15.50	15.34	15.17	15.14	14.99	14.94	14.99
	0.123	0.122	0.126	0.124	0.132	0.133	0.140	0.136	0.139	0.161	0.165	0.164	0.180

TABLE 2—*Continued*

No. (1)	03 (2)	04 (3)	05 (4)	06 (5)	07 (6)	08 (7)	09 (8)	10 (9)	11 (10)	12 (11)	13 (12)	14 (13)	15 (14)
141.....	17.93	17.56	17.20	17.00	16.63	16.52	16.33	16.20	16.09	16.00	15.88	15.73	15.70
	0.019	0.014	0.014	0.012	0.014	0.013	0.012	0.013	0.014	0.014	0.022	0.018	0.022
143.....	17.11	16.55	16.19	16.08	15.74	15.66	15.48	15.34	15.23	15.14	15.00	14.88	14.86
	0.070	0.061	0.064	0.063	0.071	0.071	0.067	0.068	0.076	0.086	0.089	0.081	0.085
144.....	17.41	16.99	16.60	16.44	16.15	16.13	15.94	15.82	15.67	15.58	15.42	15.37	15.35
	0.159	0.166	0.170	0.171	0.196	0.208	0.210	0.218	0.234	0.257	0.259	0.264	0.271
145.....	18.79	18.33	17.99	17.78	17.59	17.53	17.47	17.24	17.21	17.23	17.14	16.88	17.19
	0.188	0.178	0.179	0.166	0.199	0.195	0.218	0.200	0.237	0.294	0.307	0.255	0.350
146.....	17.89	17.41	17.11	16.98	16.70	16.65	16.50	16.32	16.18	16.08	15.95	15.91	15.87
	0.187	0.185	0.198	0.196	0.222	0.226	0.230	0.222	0.237	0.259	0.270	0.263	0.264
148.....	16.63	16.31	15.98	15.86	15.51	15.47	15.32	15.19	15.12	15.01	14.89	14.84	14.85
	0.053	0.059	0.060	0.059	0.062	0.065	0.063	0.067	0.076	0.081	0.085	0.085	0.091
149.....	18.07	17.69	17.31	17.11	16.70	16.59	16.40	16.27	16.17	16.05	15.96	15.78	15.79
	0.025	0.018	0.015	0.014	0.013	0.011	0.011	0.012	0.014	0.014	0.022	0.018	0.024
150.....	17.45	17.00	16.65	16.50	16.19	16.13	15.97	15.81	15.63	15.54	15.36	15.19	15.22
	0.070	0.062	0.061	0.057	0.061	0.060	0.058	0.058	0.060	0.066	0.067	0.058	0.062
151.....	16.11	15.59	15.16	14.91	14.49	14.39	14.13	13.99	13.80	13.68	13.53	13.43	13.39
	0.026	0.023	0.020	0.016	0.013	0.011	0.009	0.009	0.008	0.007	0.007	0.007	0.008
152.....	17.06	16.60	16.23	16.13	15.78	15.72	15.54	15.41	15.25	15.15	15.01	14.86	14.84
	0.083	0.080	0.077	0.072	0.070	0.068	0.062	0.061	0.062	0.067	0.067	0.058	0.060
153.....	17.29	16.81	16.42	16.29	15.96	15.89	15.68	15.55	15.39	15.30	15.20	15.06	15.05
	0.063	0.058	0.056	0.053	0.055	0.054	0.051	0.051	0.051	0.058	0.061	0.054	0.058
154.....	17.71	17.14	16.76	16.70	16.41	16.35	16.25	16.14	16.02	15.92	15.86	15.89	15.90
	0.096	0.085	0.083	0.085	0.091	0.092	0.096	0.098	0.107	0.118	0.125	0.140	0.150
155.....	19.00	18.53	18.22	18.00	17.70	17.65	17.40	17.27	17.12	17.08	17.01	16.69	16.67
	0.049	0.034	0.025	0.023	0.025	0.019	0.023	0.022	0.024	0.023	0.042	0.027	0.055
157.....	18.23	17.98	17.74	17.60	17.45	17.40	17.28	17.21	17.28	17.16	17.04	17.01	17.08
	0.054	0.056	0.060	0.058	0.075	0.068	0.074	0.078	0.108	0.105	0.118	0.105	0.130
158.....	15.59	15.19	14.90	14.71	14.44	14.39	14.19	14.08	14.02	13.95	13.84	13.74	13.75
	0.004	0.003	0.002	0.002	0.002	0.002	0.002	0.002	0.002	0.002	0.004	0.003	0.005
159.....	18.12	17.75	17.36	17.23	16.82	16.72	16.49	16.35	16.19	16.01	15.86	15.77	15.77
	0.037	0.032	0.026	0.025	0.021	0.019	0.020	0.020	0.021	0.019	0.023	0.044	0.050
160.....	18.48	18.25	18.09	17.94	17.80	17.62	17.68	17.51	17.59	17.62	17.39	17.28	17.44
	0.027	0.026	0.027	0.034	0.046	0.029	0.040	0.032	0.044	0.058	0.061	0.056	0.122
161.....	17.06	16.74	16.44	16.31	16.05	16.00	15.84	15.75	15.69	15.60	15.50	15.46	15.51
	0.022	0.022	0.022	0.021	0.023	0.023	0.022	0.024	0.027	0.028	0.032	0.031	0.038
162.....	18.52	18.04	17.71	17.55	17.18	17.12	16.85	16.73	16.54	16.39	16.32	15.99	15.97
	0.055	0.051	0.047	0.047	0.049	0.047	0.044	0.047	0.048	0.052	0.058	0.047	0.054
163.....	16.23	15.67	15.30	15.15	14.77	14.69	14.48	14.36	14.18	14.10	14.00	13.80	13.77
	0.006	0.004	0.004	0.004	0.004	0.004	0.004	0.004	0.004	0.004	0.005	0.005	0.006
164.....	18.85	18.31	17.99	17.86	17.46	17.45	17.38	17.08	17.00	16.86	16.85	16.59	16.60
	0.069	0.044	0.042	0.043	0.049	0.050	0.045	0.048	0.054	0.068	0.082	0.068	0.080
165.....	17.04	16.83	16.58	16.47	16.24	16.21	16.08	15.99	15.97	15.86	15.75	15.72	15.74
	0.014	0.016	0.017	0.016	0.019	0.020	0.021	0.022	0.025	0.026	0.029	0.029	0.039
166.....	17.31	17.10	16.84	16.75	16.60	16.61	16.49	16.45	16.43	16.43	16.41	16.40	16.50
	0.028	0.030	0.030	0.030	0.037	0.039	0.040	0.044	0.057	0.061	0.071	0.078	0.102
167.....	18.45	17.99	17.64	17.46	17.13	17.07	16.85	16.75	16.63	16.50	16.44	16.31	16.20
	0.058	0.058	0.056	0.053	0.060	0.058	0.059	0.061	0.066	0.072	0.079	0.075	0.078
169.....	18.48	17.82	17.31	17.23	16.86	16.78	16.55	16.41	16.25	16.10	15.97	15.88	15.82
	0.063	0.049	0.045	0.047	0.051	0.050	0.050	0.050	0.055	0.057	0.062	0.058	0.061
171.....	16.38	15.85	15.49	15.34	15.01	14.95	14.74	14.63	14.48	14.39	14.26	14.16	14.15
	0.010	0.009	0.008	0.008	0.009	0.009	0.009	0.009	0.010	0.011	0.012	0.011	0.012
172.....	17.59	17.17	16.84	16.68	16.40	16.30	16.15	16.02	15.85	15.73	15.61	15.54	15.50
	0.032	0.032	0.030	0.028	0.026	0.025	0.023	0.024	0.025	0.025	0.031	0.030	0.035
173.....	18.87	18.46	18.06	17.87	17.51	17.39	17.17	16.99	16.84	16.73	16.58	16.49	16.44
	0.169	0.164	0.146	0.125	0.114	0.101	0.088	0.080	0.083	0.078	0.078	0.084	0.090
174.....	16.63	16.18	15.82	15.62	15.22	15.14	14.96	14.84	14.67	14.54	14.51	14.39	14.33
	0.006	0.004	0.003	0.003	0.003	0.003	0.003	0.003	0.004	0.003	0.007	0.005	0.007
177.....	19.02	18.63	18.43	18.27	18.03	17.99	17.71	17.64	17.53	17.51	17.62	17.30	17.46
	0.043	0.036	0.031	0.032	0.040	0.038	0.038	0.041	0.051	0.052	0.109	0.061	0.116
178.....	15.82	15.52	15.21	15.09	14.82	14.77	14.63	14.53	14.49	14.35	14.26	14.24	14.22
	0.006	0.005	0.005	0.005	0.005	0.005	0.005	0.006	0.007	0.007	0.009	0.009	0.011
179.....	16.23	15.87	15.55	15.42	15.14	15.09	14.95	14.83	14.75	14.65	14.56	14.50	14.53
	0.014	0.013	0.014	0.013	0.014	0.014	0.015	0.015	0.017	0.018	0.019	0.019	0.022

TABLE 2—*Continued*

No. (1)	03 (2)	04 (3)	05 (4)	06 (5)	07 (6)	08 (7)	09 (8)	10 (9)	11 (10)	12 (11)	13 (12)	14 (13)	15 (14)
180.....	16.99	16.59	16.28	16.10	15.81	15.76	15.55	15.46	15.39	15.31	15.21	15.13	15.14
	0.008	0.006	0.005	0.005	0.006	0.004	0.005	0.005	0.007	0.007	0.012	0.010	0.015
181.....	17.79	17.40	17.06	16.96	16.58	16.54	16.34	16.28	16.15	16.03	15.93	15.84	15.81
	0.038	0.030	0.026	0.028	0.026	0.025	0.022	0.026	0.030	0.028	0.035	0.033	0.039
182.....	16.43	16.05	15.73	15.50	15.18	15.12	14.88	14.76	14.67	14.58	14.45	14.33	14.29
	0.006	0.004	0.004	0.004	0.004	0.004	0.004	0.004	0.005	0.005	0.007	0.006	0.008
183.....	17.06	16.57	16.27	16.08	15.78	15.72	15.49	15.36	15.27	15.19	15.12	14.95	14.96
	0.007	0.004	0.003	0.004	0.004	0.004	0.004	0.004	0.004	0.003	0.009	0.005	0.010
185.....	16.56	16.11	15.79	15.62	15.32	15.27	15.07	14.96	14.85	14.73	14.64	14.57	14.56
	0.007	0.006	0.005	0.005	0.006	0.006	0.006	0.007	0.008	0.008	0.009	0.009	0.012
184.....	18.66	18.06	17.56	17.47	17.01	16.92	16.69	16.62	16.35	16.21	16.17	15.99	15.93
	0.051	0.036	0.029	0.028	0.024	0.023	0.021	0.024	0.023	0.023	0.034	0.029	0.033
186.....	19.82	18.84	18.52	18.34	17.99	17.79	17.50	17.45	17.07	17.01	16.99	16.59	16.49
	0.109	0.058	0.050	0.045	0.048	0.036	0.035	0.040	0.034	0.038	0.052	0.038	0.047
187.....	18.25	17.98	17.41	17.29	16.93	16.83	16.53	16.46	16.42	16.23	16.13	16.03	16.01
	0.055	0.049	0.043	0.036	0.035	0.031	0.027	0.028	0.031	0.032	0.048	0.040	0.047
188.....	17.71	17.58	17.39	17.30	17.01	16.96	16.78	16.67	16.56	16.42	16.31	16.18	16.15
	0.080	0.081	0.089	0.082	0.075	0.075	0.062	0.063	0.058	0.055	0.050	0.051	0.060
189.....	18.41	17.80	17.39	17.21	16.77	16.69	16.51	16.37	16.17	16.06	16.05	15.80	15.75
	0.031	0.020	0.016	0.015	0.017	0.015	0.016	0.017	0.018	0.020	0.022	0.021	0.025
190.....	17.78	17.40	17.08	16.93	16.60	16.54	16.37	16.25	16.12	16.02	16.01	15.88	15.82
	0.016	0.012	0.010	0.009	0.014	0.012	0.013	0.014	0.016	0.016	0.022	0.025	0.030
192.....	18.33	18.20	18.08	18.02	17.89	17.96	18.04	17.99	17.99	17.84	18.11	18.23	18.20
	0.038	0.033	0.037	0.038	0.049	0.052	0.066	0.073	0.084	0.091	0.167	0.182	0.212
194.....	17.92	17.62	17.36	17.22	16.99	16.95	16.78	16.63	16.69	16.60	16.53	16.47	16.46
	0.017	0.014	0.012	0.013	0.015	0.013	0.015	0.015	0.018	0.018	0.032	0.025	0.042
193.....	16.58	16.01	15.68	15.51	15.12	15.03	14.85	14.73	14.54	14.40	14.42	14.29	14.18
	0.010	0.005	0.004	0.004	0.004	0.004	0.004	0.004	0.004	0.004	0.006	0.005	0.007
197.....	19.01	18.40	18.01	17.85	17.41	17.35	17.08	16.95	16.71	16.59	16.47	16.29	16.24
	0.090	0.068	0.061	0.056	0.052	0.051	0.045	0.046	0.047	0.043	0.051	0.049	0.056
198.....	18.42	18.16	17.78	17.65	17.36	17.30	17.17	17.08	16.93	16.83	16.80	16.76	16.67
	0.061	0.047	0.043	0.037	0.042	0.043	0.042	0.045	0.056	0.054	0.070	0.065	0.073
200.....	19.60	19.20	18.87	18.64	18.22	18.09	17.88	17.77	17.60	17.47	17.23	17.36	17.26
	0.217	0.186	0.170	0.139	0.124	0.110	0.097	0.098	0.101	0.096	0.093	0.130	0.145
201.....	16.85	16.56	16.28	16.14	15.87	15.82	15.64	15.55	15.46	15.37	15.14	15.25	15.25
	0.009	0.008	0.007	0.008	0.008	0.007	0.008	0.010	0.010	0.011	0.013	0.012	0.018
203.....	17.67	17.25	16.90	16.76	16.45	16.36	16.18	16.06	15.94	15.85	15.76	15.74	15.70
	0.019	0.015	0.013	0.013	0.012	0.011	0.012	0.011	0.015	0.012	0.021	0.019	0.024
204.....	16.66	16.23	15.92	15.77	15.45	15.39	15.21	15.17	14.98	14.86	14.82	14.73	14.70
	0.007	0.005	0.004	0.004	0.005	0.004	0.005	0.006	0.007	0.005	0.009	0.007	0.011
205.....	16.32	15.94	15.67	15.52	15.23	15.24	15.01	14.90	14.78	14.69	14.63	14.53	14.52
	0.007	0.005	0.005	0.005	0.005	0.005	0.006	0.005	0.006	0.006	0.009	0.008	0.011
206.....	15.92	15.54	15.25	15.13	14.82	14.87	14.86	14.50	14.42	14.32	14.29	14.20	14.20
	0.005	0.004	0.004	0.003	0.004	0.004	0.005	0.004	0.005	0.004	0.007	0.007	0.008
208.....	18.82	18.33	18.02	17.82	17.51	17.43	17.20	17.11	16.94	16.79	16.78	16.61	16.72
	0.038	0.030	0.026	0.025	0.030	0.025	0.028	0.030	0.032	0.027	0.048	0.039	0.067
209.....	17.48	17.11	16.78	16.68	16.43	16.32	16.15	16.08	15.97	15.88	15.93	15.80	15.78
	0.012	0.009	0.011	0.010	0.013	0.011	0.013	0.014	0.017	0.017	0.029	0.023	0.033
210.....	17.92	17.92	17.66	17.58	17.37	17.33	17.21	17.08	16.99	16.94	16.83	16.78	16.87
	0.022	0.023	0.020	0.022	0.023	0.022	0.028	0.027	0.033	0.030	0.048	0.041	0.067
211.....	17.30	17.06	16.79	16.67	16.39	16.38	16.23	16.13	16.06	15.95	15.89	15.86	15.87
	0.015	0.012	0.011	0.011	0.012	0.011	0.013	0.013	0.016	0.015	0.024	0.018	0.031
213.....	17.92	17.42	17.13	16.94	16.79	16.51	16.40	16.31	16.08	15.93	15.99	15.84	15.77
	0.027	0.022	0.020	0.017	0.023	0.017	0.019	0.018	0.019	0.018	0.026	0.024	0.028
214.....	18.32	18.11	17.84	17.79	17.55	17.44	17.26	17.25	17.05	17.00	16.88	16.93	17.06
	0.037	0.037	0.038	0.038	0.043	0.038	0.037	0.043	0.048	0.047	0.064	0.067	0.097
215.....	18.26	17.80	17.44	17.28	16.95	16.90	16.69	16.59	16.42	16.32	16.29	16.12	16.07
	0.024	0.023	0.021	0.022	0.022	0.022	0.018	0.023	0.023	0.023	0.032	0.030	0.040
216.....	17.53	17.39	17.29	17.27	17.14	17.14	17.14	17.11	17.03	17.02	17.18	17.02	16.91
	0.023	0.024	0.027	0.027	0.035	0.038	0.042	0.045	0.056	0.058	0.086	0.078	0.087
362.....	18.45	17.99	17.74	17.67	17.38	17.35	17.26	17.24	17.22	17.08	17.13	17.05	17.00
	0.026	0.021	0.018	0.019	0.024	0.020	0.023	0.026	0.037	0.037	0.059	0.052	0.081
217.....	17.52	17.07	16.74	16.58	16.26	16.20	16.02	15.90	15.78	15.66	15.64	15.55	15.55
	0.014	0.009	0.007	0.008	0.010	0.008	0.009	0.010	0.011	0.009	0.015	0.016	0.025

TABLE 2—*Continued*

No. (1)	03 (2)	04 (3)	05 (4)	06 (5)	07 (6)	08 (7)	09 (8)	10 (9)	11 (10)	12 (11)	13 (12)	14 (13)	15 (14)
218.....	15.67	15.28	14.99	14.83	14.54	14.49	14.30	14.20	14.09	13.96	13.93	13.85	13.82
	0.005	0.003	0.003	0.003	0.003	0.003	0.003	0.003	0.003	0.003	0.004	0.004	0.005
220.....	17.40	17.08	16.77	16.68	16.36	16.33	16.20	16.14	16.04	15.92	15.91	15.86	15.87
	0.015	0.013	0.012	0.012	0.013	0.012	0.013	0.013	0.016	0.014	0.019	0.022	0.030
221.....	17.86	17.38	17.08	16.92	16.53	16.48	16.30	16.18	16.03	15.90	15.85	15.83	15.75
	0.016	0.012	0.011	0.010	0.010	0.009	0.010	0.011	0.014	0.011	0.019	0.019	0.025
222.....	18.20	17.82	17.64	17.50	17.28	17.26	17.08	17.00	16.86	16.82	16.77	16.58	16.51
	0.021	0.014	0.013	0.013	0.016	0.015	0.016	0.018	0.020	0.017	0.032	0.024	0.044
223.....	17.56	17.49	17.33	17.34	17.23	17.21	17.20	17.20	17.10	17.14	17.17	17.12	17.21
	0.022	0.026	0.029	0.026	0.033	0.032	0.039	0.040	0.049	0.047	0.073	0.074	0.118
224.....	16.22	15.92	15.67	15.54	15.28	15.24	15.10	15.02	14.92	14.83	14.80	14.77	14.76
	0.005	0.004	0.003	0.003	0.004	0.003	0.004	0.004	0.005	0.004	0.007	0.007	0.010
225.....	15.17	14.69	14.40	14.24	13.89	13.83	12.80	13.53	13.36	13.26	13.22	13.12	13.06
	0.004	0.003	0.003	0.002	0.002	0.002	0.001	0.002	0.002	0.002	0.003	0.002	0.003
228.....	17.96	17.44	17.09	16.92	16.55	16.44	16.25	16.13	15.95	15.82	15.85	15.75	15.67
	0.016	0.009	0.008	0.007	0.008	0.007	0.007	0.009	0.010	0.009	0.017	0.015	0.020
229.....	17.37	17.07	16.81	16.69	16.41	16.37	16.22	16.14	16.01	15.93	15.93	15.90	15.85
	0.014	0.011	0.011	0.010	0.011	0.010	0.009	0.010	0.012	0.011	0.020	0.017	0.025
231.....	18.14	17.76	17.45	17.36	16.98	16.94	16.79	16.70	16.58	16.46	16.44	16.39	16.35
	0.033	0.023	0.019	0.020	0.021	0.018	0.020	0.020	0.025	0.025	0.041	0.037	0.046
234.....	17.67	17.33	17.03	16.86	16.56	16.50	16.25	16.23	16.07	15.92	15.94	15.87	15.78
	0.046	0.030	0.027	0.020	0.019	0.018	0.020	0.015	0.015	0.015	0.017	0.019	0.029
235.....	17.18	16.84	16.56	16.40	16.10	16.02	15.85	15.78	15.53	15.39	15.40	15.32	15.22
	0.019	0.013	0.012	0.010	0.009	0.008	0.008	0.008	0.008	0.007	0.012	0.012	0.016

BATC photometric values minus the values of Battistini et al.) are $\langle \Delta V \rangle = -0.083 \pm 0.069$ and $\langle \Delta(B-V) \rangle = -0.128 \pm 0.096$ (excluding objects mentioned above) and between the BATC photometry and Barmby et al. (2000) are $\langle \Delta V \rangle = 0.063 \pm 0.065$ and $\langle \Delta(B-V) \rangle = 0.067 \pm 0.090$, respectively. The uncertainties in B (BATC) and V (BATC) were determined linearly, i.e., $\sigma_B = \sigma_{04} + 0.2218(\sigma_{03} + \sigma_{05})$ and $\sigma_V = \sigma_{07} + 0.3233(\sigma_{06} + \sigma_{08})$, to reflect photometric errors in the six filter bands. For the colors, we calculated their errors by $\sigma_{B-V} = (\sigma_B^2 + \sigma_V^2)^{1/2}$. From these two figures, we can see that our results are in better agreement with Barmby et al. (2000) than with Battistini et al. (1987).

3. DATABASES OF SIMPLE STELLAR POPULATIONS

An SSP is defined as a single generation of coeval stars with fixed parameters such as metal abundance, initial mass function, etc. (Buzzoni 1997). In evolutionary synthesis models, they are modeled by a collection of evolutionary

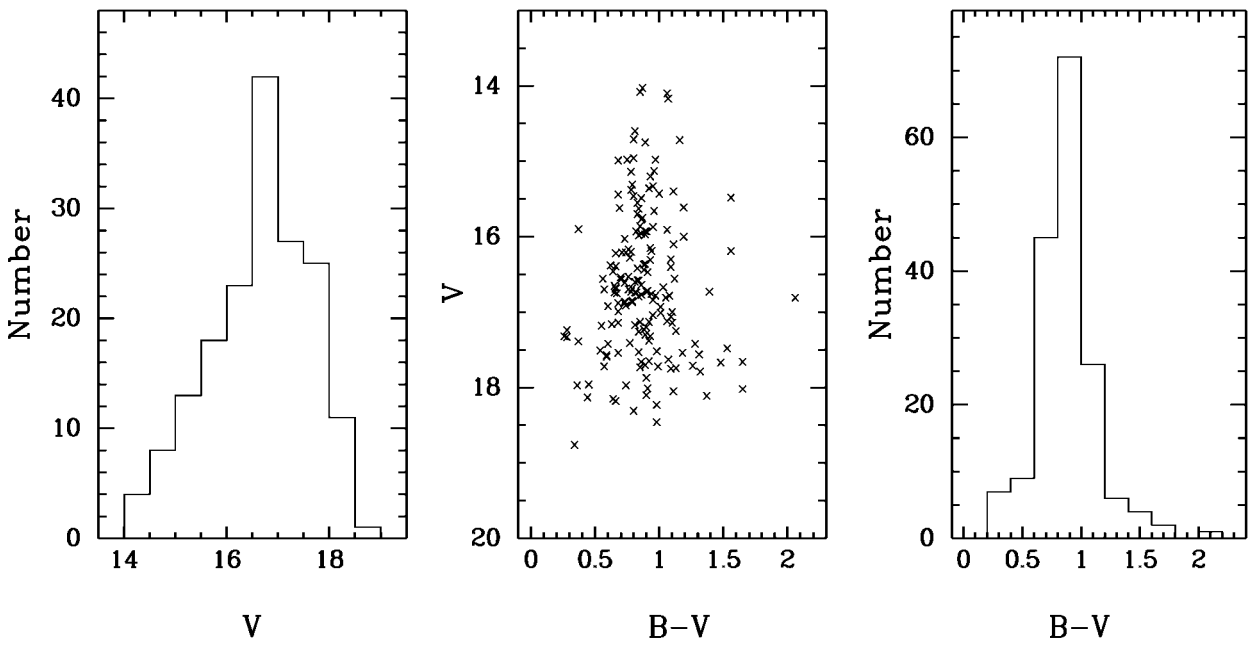

FIG. 1.—Histograms of the computed V magnitudes and $B-V$ colors and the color-magnitude diagram for 172 GCs

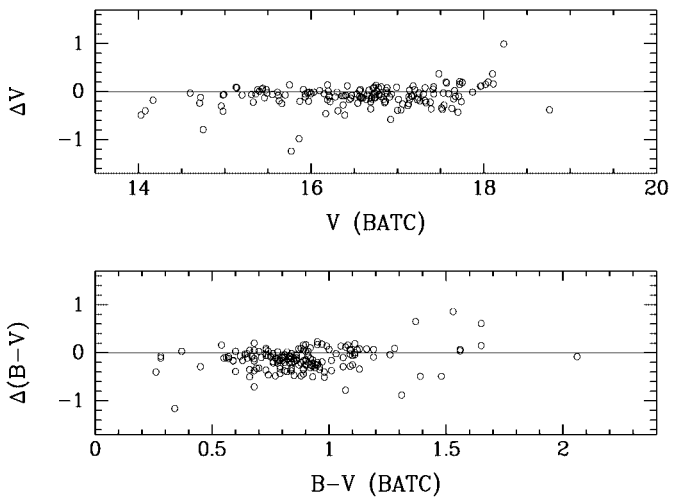

FIG. 2.—Comparison of GC photometry with Battistini et al. (1987). The vertical axis is the BATC photometry minus the measurement of Battistini et al. (1987).

tracks of stars with different masses and initial chemical components and a set of stellar spectra at different evolutionary stages. Because SSPs are the basic building elements for synthetic spectra of galaxies, we can infer the formation and evolution of the parent galaxies from them (Jablonka et al. 1996). Since Tinsley (1972) and Searle, Sargent, & Bagnuolo (1973) did the pioneering work in evolutionary population synthesis, this method has become a standard technique to study the stellar populations of galaxies. A broad variety of empirical and theoretical database has been built up, and a comprehensive library of models has been compiled (Leitherer et al. 1996). Widely used models are from GISSEL96 (Charlot & Bruzual 1991; Bruzual & Charlot 1993; G. Bruzual & S. Charlot 1996, unpublished), the Padova and Geneva group (e.g., Schaerer & de Koter 1997; Schaerer & Vacca 1998; Bressan et al. 1996; Chiosi et al. 1998), PEGASE (Fioc & Rocca-Volmerange 1997), and STARBURST99 (Leitherer et al. 1999). In the current paper, we will use the GSSPs to estimate the ages of the sample GCs, since they are simple and well explored.

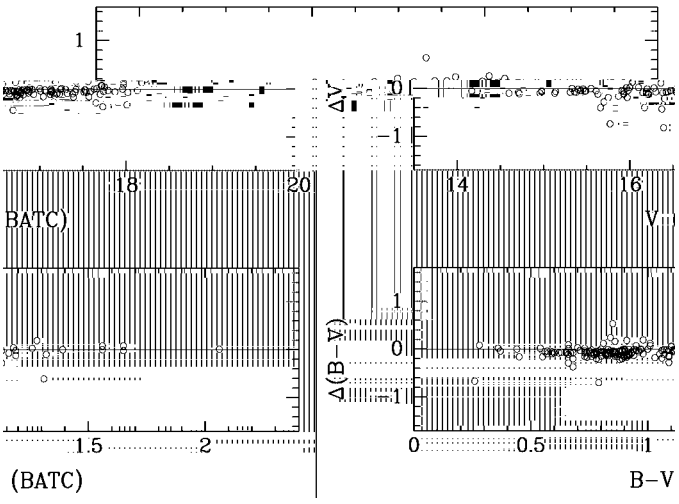

FIG. 3.—Comparison of GC photometry with Barmby et al. (2000). The vertical axis is the BATC photometry minus the measurement of Barmby et al. (2000).

3.1. *SED of GSSPs*

GSSPs method, which is based on a model of stellar population synthesis developed by Charlot & Bruzual (1991), can be used to determine the distribution of stars in the theoretical color-magnitude diagram for any stellar system. The updated GSSPs synthesis model (G. Bruzual & S. Charlot 1996, unpublished), which was upgraded from the Bruzual & Charlot (1993) version, provides the evolution of the spectra photometric properties for a wider range of stellar metallicities, with $Z = 0.0004$, 0.004, 0.008, 0.02, 0.05, and 0.1. The chemical parameters follow the helium-to-metal enrichment law $dY/dZ = 2.5$, and the initial mass function obeys the Salpeter (1955) law with $\alpha = 2.35$ (Leitherer et al. 1996).

3.2. *Integrated Colors of GSSPs*

To obtain the age, metallicity, and interstellar medium reddening distribution for M81, Kong et al. (2000) found the best match between the intrinsic colors and the predictions of GSSP for each cell of M81. To estimate the ages for the sample clusters in this paper, we follow the method of Kong et al. (2000). Since the observational data are integrated luminosity, as Kong et al. (2000) and Ma et al. (2002b) did, we convolve the SED of GSSP with the BATC filter profiles to obtain the optical and near-infrared integrated luminosity for comparisons. The integrated luminosity $L_{\lambda_i}(t, Z)$ in the ith BATC filter can be calculated with

$$L_{\lambda_i}(t, Z) = \frac{\int F_\lambda(t, Z)\varphi_i(\lambda)d\lambda}{\int \varphi_i(\lambda)d\lambda} , \qquad (3)$$

where $F_\lambda(t,Z)$ is the SED of the GSSP of metallicity Z at age t, and $\varphi_i(\lambda)$ is the response function in the ith filter of the BATC filter system ($i = 3, 4, \ldots, 15$), respectively. To avoid using parameters that are dependent on the distance, we calculate the integrated colors of a GSSP relative to the BATC filter BATC08 ($\lambda = 6075$ Å):

$$C_{\lambda_i}(t, Z) = L_{\lambda_i}(t, Z)/L_{6075}(t, Z) . \qquad (4)$$

Finally, using equations (3) and (4), we obtained the intermediate-band colors of a GSSP for six metallicities from $Z = 0.0004$ to 0.1.

4. REDDENING CORRECTION

The SED of a stellar system will be affected by age, metallicity, and reddening along the line of sight. Generally, older age, higher metallicity, and larger reddening all lead to redder SEDs of stellar systems in the optical (Bressan et al. 1996; Mollà, Ferrini, & Diaz 1997), and these effects are difficult to separate (Calzetti 1997; Vazdekis et al. 1997; Origlia et al. 1999). In order to estimate the ages for 172 GCs, the intrinsic colors of these GCs should be obtained. The observed colors are mainly affected by two sources of reddening: the foreground extinction in the Milk Way and internal reddening in M31.

The Galactic reddening in the direction of M31 was estimated by many authors (e.g., van den Bergh 1969; McClure & Racine 1969; Frogel et al. 1980), and the sim-

ilar values of the foreground color excess, $E(B-V)$, were determined, such as $E(B-V) = 0.08$ given by van den Bergh (1969), 0.11 given by McClure & Racine (1969), and 0.08 given by Frogel et al. (1980). As Crampton et al. (1985) did, we use the value of 0.10 as the foreground color excess.

The reddening of GCs in M31 has been determined by several ways in previous studies. As is mentioned, Vetešník (1962a) compiled a comprehensive catalog of 257 GC candidates and derived color excesses for the candidates that were considered to be most probably the GCs (Vetešník 1962b). To obtain true colors of the clusters, Vetešník (1962b) calculated the average true color index of 36 GCs beyond the body of M31, and considered the result, $B-V = 0.83$ mag, as the uniform value of true color for all GCs in M31. Actually, this implicated that these clusters were only affected by the foreground Galactic extinction. Later, many authors used this assumption of a single intrinsic color for all GCs in M31 (Bajaja & Gergely 1977; Iye & Richter 1985).

Using the slope parameter, S, Crampton et al. (1985) calculated intrinsic colors for individual GCs. S, defined by Hartwick (1968), was proved to be a good indicator of intrinsic color and metallicity. From the derived relationship between $(B-V)_0$ and S, Crampton et al. (1985) gave intrinsic colors and color excesses for most candidates in their catalog.

A comprehensive list of colors and metallicities for the M31 GCs was given by Barmby et al. (2000). In order to determine the cluster reddening, they set two reasonable assumptions that both the extinction law and the GC intrinsic color were the same. By using the color-metallicity relationships and the relationships between colors and reddening-free parameters, two basic methods were used independently to obtain the intrinsic colors. Finally, for each GC, the two results were combined by their own weight.

In present paper, we mainly use color excesses given by Barmby et al. (2000) for reddening correction. Since our sample contains a total of 172 GCs and values of $E(B-V)$ for only 152 of 172 objects were derived by Barmby et al. (2000), there remains 20 objects undetermined. We note that values of S, the slope parameter, for nine of these 20 GCs were given by Crampton et al. (1985), the intrinsic colors for these nine GCs can be derived from the equation given by Crampton et al. (1985),

$$(B-V)_0 = 0.066S - 0.17(B-V) + 0.32 , \qquad (5)$$

where the values of S are taken from Crampton et al. (1985) and values of $B-V$ comes from Barmby et al. (2000). At last, there are still 11 GCs whose color excesses are not determined. For these 11 objects, we assume that they are only affected by the foreground Galactic extinction and their color excesses are the foreground color excess, i.e., $E(B-V) = 0.10$. In addition, we adopted the extinction curve presented by Zombeck (1990). An extinction correction, $A_\lambda = R_\lambda E(B-V)$, was applied, where R_λ is obtained by interpolating using the data of Zombeck (1990).

5. AGE ESTIMATES

After the photometric measurements are dereddened, intrinsic colors for each GC depend on two parameters, age and metallicity, since we model the stellar populations of the GCs by SSPs. In this section, we will determine the ages and best-fit model of metallicity for our sample GCs simultaneously by the least-square method. The age and best-fit models of metallicity are found by minimizing the difference between the intrinsic colors of the sample GCs and integrated colors of GSSP:

$$R^2(n,t,Z) = \frac{\sum_{i=3}^{15}[C_{\lambda_i}^{\rm intr}(n) - C_{\lambda_i}^{\rm ssp}(t,Z)]^2/\sigma_i^2}{\sum_{i=3}^{15} 1/\sigma_i^2} , \qquad (6)$$

where $C_{\lambda_i}^{\rm ssp}(t,Z)$ is the integrated color in the ith filter of a SSP at age t in the model of metallicity Z, and $C_{\lambda_i}^{\rm intr}(n)$ presents the intrinsic integrated color in the same filter of the nth GC. The differences are weighted by $1/\sigma_i^2$, where the σ_i's are observational uncertainties of the passbands. The M31 GCs generally have a metal abundance, [Fe/H], lower than 0.0 (Barmby et al. 2000), which corresponds to $Z = 0.0169$ (Leitherer et al. 1996), so we only select the models of three metallicities, 0.0004, 0.004, and 0.02, of GSSP.

Figure 4 shows the fit of the integrated color of an SSP ($Z = 0.0004$, 0.004, and 0.02) with the intrinsic color for 20 GCs selected from the 172 GCs (the first 20 GCs in Table 2). In Figure 4, filled circle represents the intrinsic integrated color of a GC, and the thick line represents the best fit of the integrated color of a SSP of the GSSP. From Figure 4, we see that SEDs of GCs are fitted very well by the best-fit SSP of GSSP model. Table 3 presents ages and the best-fit models of metallicities for all the 172 GCs. The uncertainties in the age estimates arising from photometric uncertainties are 0.2 or so, i.e., age $\pm$ (0.2 $\times$ age) [log yr]. In addition, we noted that clusters 127 and 225 have strong emission lines in the filter of BATC09, so we did not use the color of this filter in the process of fitting.

We should emphasize that, in this study, we estimate the ages of our sample clusters by comparing the photometry of each object with models for different values of metallicity as Chandar, Bianchi, & Ford (1999a, 1999b, 2001) did. Recently, using the similar technique, Ma et al. (2002a) estimated ages of 10 halo GCs in M33 with four models of metallicities ($Z = 0.0004$, 0.004, 0.008, and 0.02). Here we use three metallicity models to estimate ages for our sample GCs. In each model, the ages of SSPs are from 0 to 20 Gyr. We should also emphasize that, for very old GCs, the age/metallicity degeneracy becomes pronounced. In this case, we only mean that in some model of metallicity, the intrinsic integrated color of a GC can do the best fit with the integrated color of a SSP at some age.

From Table 3, we see that most GCs are old objects, except clusters 133 and 362. Cluster 133 appears to be very young, and its reddening-corrected SED significantly differs from others'. This case can be explained by the high value of $E(B-V)$. Since $E(B-V)$ of cluster 133 was not given by Barmby et al. (2000), we calculated its value using S (see § 4). According to equation (5), $E(B-V)$ is determined as follows:

$$E(B-V) = 1.17(B-V) - 0.066S - 0.32 , \qquad (7)$$

where $B-V$ comes from Barmby et al. (2000), and S from Crampton et al. (1985), as has been described in § 4. From equation (7), we can see that a high value of $B-V$ and a small value of S all lead to high $E(B-V)$. In addition, we should note that the value of $B-V$ of cluster 133 given by Barmby et al. (2000) is 0.93, while the corre-

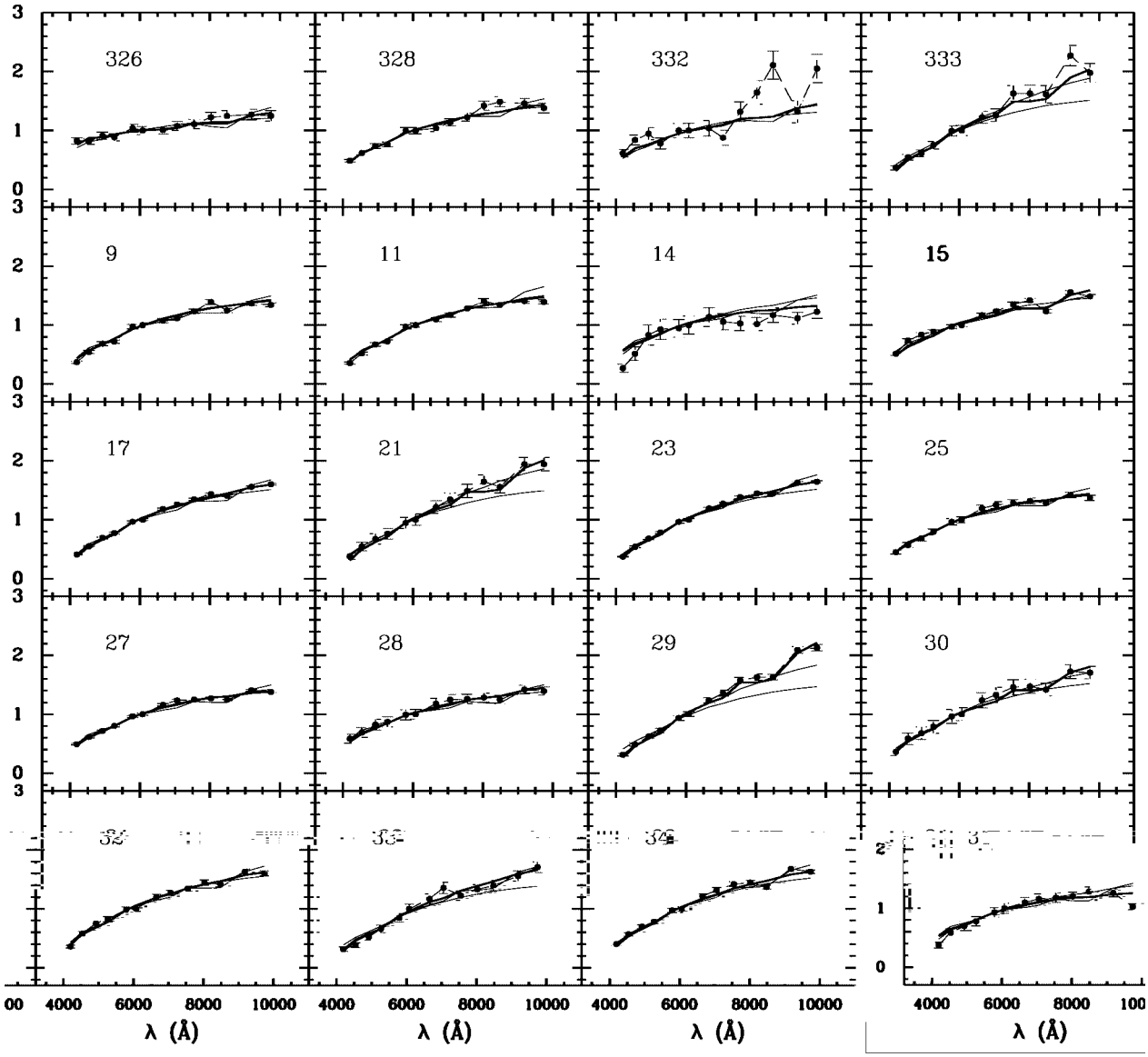

FIG. 4.—Map of the fit of the integrated color of a SSP ($Z = 0.0004$, 0.004, and 0.02) with intrinsic integrated color for 20 GCs selected from the 172 GCs (the first 20 GCs in Table 2). Filled circles represent the intrinsic integrated color of a GC, the thick line represents the best fit of the integrated color of a SSP of GSSP, and the thin lines represent the other two fits. The Y-axis is the ratio of the flux in each filter to the flux in filter BATC08.

sponding values given by Battistini et al. (1987) and the BATC photometry are 0.66 and 0.26, respectively. The value of S given by Crampton et al. (1985) is very low, -4, while values of most S are more than 0. Due to these two reasons, or perhaps one of the two reasons, cluster 133 appears very young. Another "young" cluster is cluster 362, whose $E(B-V)$ given by Barmby et al. (2000) is 0.42, but the uncertainty of $E(B-V)$ is 0.45. Perhaps due to the big uncertainty of $E(B-V)$, cluster 362 also appears very young. In the next analysis, we do not include these two GCs.

Figure 5 plots histograms of GC ages for three models of different metallicities, $Z = 0.02$, 0.004, and 0.0004, and for all GCs, except clusters 133 and 362. From this figure, we can see that almost all these GCs have ages more than 10^9 yr, and most of them are around 10^{10} yr old. In the separated histograms of three models, only a few GCs are included in the $Z = 0.02$ model, while most GCs are included in the $Z = 0.004$ and 0.0004 models. We can also see that ages in the $Z = 0.004$ and 0.0004 models have apparently different distributions. The peak of age in the $Z = 0.004$ model is at about 6 Gyr, while the peak in the $Z = 0.0004$ model is about 19 Gyr. This means, in general, GCs in the $Z = 0.0004$ model are older than those in the $Z = 0.004$ model.

Barmby & Huchra (2000) compared simple stellar population colors of three population synthesis models with the intrinsic colors of Galactic and M31 GCs in *UBVRIJHK* colors. They found that higher metallicity cluster colors are best fitted by the younger models, and lower metallicity cluster colors are best fitted by the older models. Our results in this paper are in agreement with Barmby & Huchra (2000).

It is well known that the abundance distributions of GCs in many galaxies are bimodal, including the M31 GC system (e.g., Barmby et al. 2000; Perrett et al. 2002). Forbes, Brodie, & Grillmair (1997) found that the metal-rich GCs in elliptical and cD galaxies are closely coupled to their parent galaxies, but the metal-poor GCs are largely independent of the galaxies. They concluded that

TABLE 3
AGE DISTRIBUTION OF 172 GCs

No.	Metallicity (Z)	Age ([log yr])	No.	Metallicity (Z)	Age ([log yr])	No.	Metallicity (Z)	Age ([log yr])
326	0.00400	8.806	93	0.00400	10.279	164	0.02000	9.009
328	0.00400	9.301	94	0.02000	9.362	165	0.00400	9.322
332	0.00400	9.057	96	0.00400	10.297	166	0.00040	9.301
333	0.02000	9.544	97	0.00040	9.796	167	0.00400	10.155
9	0.00040	10.068	98	0.00040	10.196	169	0.00400	9.322
11	0.00040	10.248	99	0.00400	9.322	171	0.00400	10.155
14	0.00040	9.574	101	0.02000	9.301	172	0.00400	9.954
15	0.02000	9.009	103	0.00400	10.130	173	0.00040	9.574
17	0.00400	9.720	102	0.00040	9.699	174	0.00040	10.130
21	0.02000	9.544	104	0.00040	9.574	177	0.00040	9.875
23	0.00400	9.813	105	0.00400	9.796	178	0.00040	10.279
25	0.00040	9.978	106	0.00400	9.796	179	0.00040	10.301
27	0.00040	9.875	108	0.00400	8.957	180	0.00040	10.041
28	0.00400	9.155	107	0.00040	9.875	181	0.00400	9.477
29	0.02000	9.942	109	0.02000	9.544	182	0.00400	9.720
30	0.02000	9.279	111	0.00040	10.196	183	0.00400	10.000
31	0.00040	9.602	110	0.00400	9.574	185	0.00400	9.760
32	0.00400	9.677	112	0.02000	9.860	184	0.00400	9.477
33	0.00400	10.146	114	0.02000	9.107	186	0.02000	10.301
34	0.00400	9.778	117	0.00040	10.033	187	0.00040	10.090
36	0.00400	10.130	115	0.00400	10.297	188	0.00400	10.283
37	0.00400	9.966	116	0.00400	9.978	189	0.02000	9.845
38	0.00400	9.322	118	0.00040	9.740	190	0.00400	9.813
39	0.00400	9.796	122	0.00400	10.301	192	0.00040	9.255
41	0.00400	10.013	123	0.00400	9.929	194	0.00040	10.301
42	0.00040	10.267	125	0.00040	9.796	193	0.00400	10.301
44	0.00040	10.267	126	0.00040	10.297	197	0.00040	9.057
48	0.00400	9.398	127	0.00400	9.813	198	0.00400	9.889
51	0.00400	9.889	353	0.02000	10.301	200	0.00040	9.875
53	0.00400	9.439	128	0.00040	10.301	201	0.00400	9.778
54	0.02000	9.107	130	0.00040	10.041	203	0.00040	10.297
56	0.02000	9.439	131	0.00400	10.283	204	0.00400	9.574
57	0.00040	9.778	133	0.00040	6.340	205	0.00400	9.740
59	0.00400	9.740	134	0.00400	9.813	206	0.00400	9.628
60	0.00040	9.760	135	0.00400	9.477	208	0.00400	9.845
61	0.02000	9.362	136	0.00040	9.155	209	0.00400	9.677
63	0.00400	9.845	137	0.00400	9.574	210	0.00400	9.107
64	0.00040	10.279	138	0.00400	9.929	211	0.00040	10.301
67	0.00040	9.544	141	0.00400	9.439	213	0.00400	9.628
68	0.00400	9.574	143	0.00400	10.155	214	0.00040	10.283
69	0.00400	9.279	144	0.00400	10.021	215	0.00400	10.061
70	0.00400	9.544	145	0.02000	10.272	216	0.00040	8.957
71	0.00400	10.301	146	0.02000	9.279	362	0.00040	6.620
72	0.00400	10.297	148	0.00040	10.176	217	0.00400	9.720
73	0.00400	9.845	149	0.00040	9.929	218	0.00040	10.301
75	0.00040	9.760	150	0.02000	9.255	220	0.00040	10.079
76	0.00040	9.740	151	0.00400	9.860	221	0.00040	10.301
77	0.00040	10.137	152	0.02000	9.362	222	0.02000	9.107
78	0.02000	10.272	153	0.00400	10.301	223	0.00040	8.806
79	0.00400	9.602	154	0.00040	9.255	224	0.00040	9.860
80	0.02000	10.297	155	0.02000	9.477	225	0.00400	9.966
82	0.00400	9.796	157	0.00040	9.544	228	0.00400	10.090
84	0.02000	10.301	158	0.00400	9.699	229	0.00400	9.699
86	0.00040	9.903	159	0.00040	10.301	231	0.00400	9.929
88	0.00040	10.021	160	0.00400	9.255	234	0.00400	9.628
90	0.02000	9.009	161	0.00040	10.155	235	0.00400	9.778
91	0.00040	9.207	162	0.02000	9.342			
92	0.00040	9.720	163	0.00400	10.301			

the metal-poor GCs are formed during the beginning of galaxy formation, and the metal-rich GCs are formed at a later stage than metal-poor GCs. If so, this may imply that the age distribution of GCs should be bimodal or multimodal. Due to our incomplete sample, from Figure 5 we cannot confirm whether or not the age distribution is bimodal or multimodal; however, we can say that the age distribution of GCs in M31 is not monomodel.

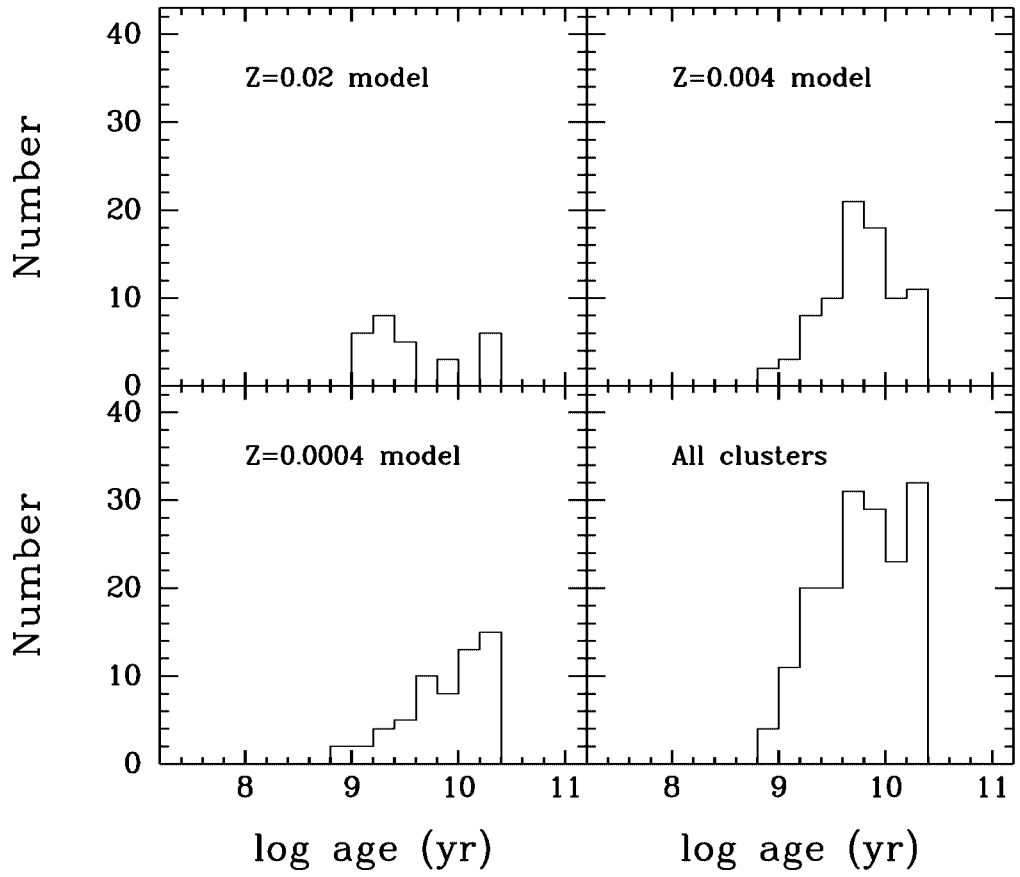

FIG. 5.—Histograms of M31 GC ages

The presence of groups of clusters in space and in age is interesting. We show the GC age as a function of galactocentric distance R in Figure 6. The galactocentric distance R for M31 GCs is derived using the distance modulus of 24.47 (Holland 1998; Stanek & Garnavich 1998), the inclination angle of 77° (Williams & Hodge 2001), and the position angle of 38° (Williams & Hodge 2001). Figure 6 shows that there exits a few groups of clusters that are nearby in space and in age. This result tells us that some nearby GCs formed simultaneously. We also plot age versus reddening-corrected apparent magnitude in Figure 7; no trend is obvious.

6. SUMMARY

In the current paper, we obtained for the first time the SEDs for 172 GCs of M31 in 13 intermediate-band filters

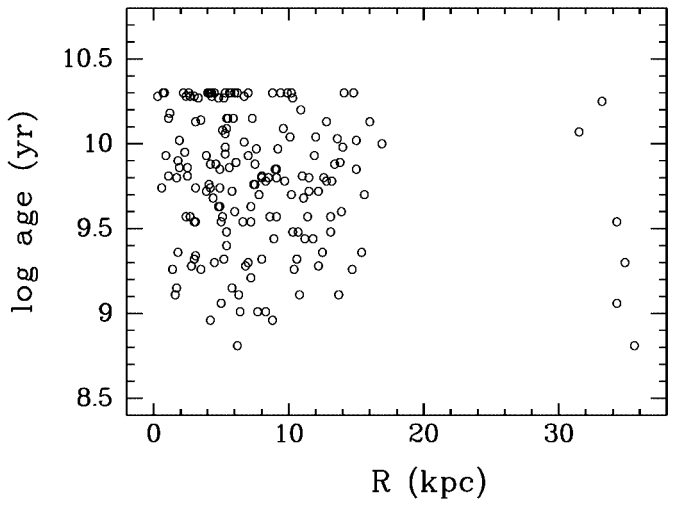

FIG. 6.—Age as a function of galactocentric distance for M31 GCs. The absence of GCs with 20 kpc $< R <$ 30 kpc is a selection effect.

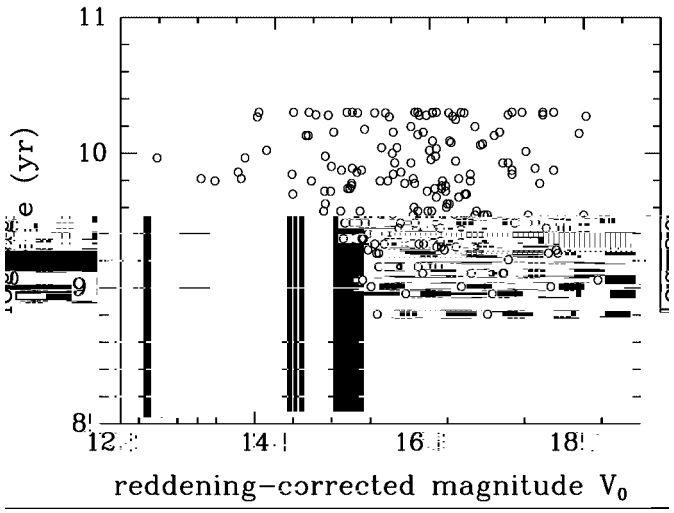

FIG. 7.—Age as a function of reddening-corrected magnitude V_0 for M31 GCs.

with the BATC 60/90 cm Schmidt telescope. The main results and conclusions are summarized as follows:

1. Using the images obtained with the BATC Multicolor Sky Survey Telescope, we obtained SEDs for 172 GCs of M31 selected from the Bologna catalog in 13 intermediate-band filters covering a range of wavelength from 3800 to 10,000 Å.

2. Using the relationship between the BATC intermediate-band system and the *UBVRI* broadband system, we derived the magnitudes in the B and V bands. The computed V and $B-V$ are in agreement with previous measurements.

3. By comparing the photometry of each GC with theoretical stellar population synthesis models, we estimated ages of the sample GCs for different metallicities. The results show that nearly all the GCs have ages more than 10^9 yr, and GCs in the metal-poor model are generally older than ones in the metal-rich model.

We would like to thank the anonymous referee for his/her insightful comments and suggestions that improved this paper. We are grateful to P. Barmby and J. P. Huchra for providing us with the values of $E(B-V)$ for GCs in M31 that they derived. We would like to thank the Padova group for providing us with a set of theoretical isochrones and SSPs. We are also indebted to G. Bruzual and S. Charlot for sending us their latest calculations of SSPs and for explanations of their code. The work is supported partly by the National Sciences Foundation under the contract Nos. 19833020 and 19503003. The BATC Survey is supported by the Chinese Academy of Sciences, the Chinese National Natural Science Foundation, and the Chinese State Committee of Sciences and Technology. The project is also supported in part by the National Science Foundation (grant INT 93-01805) and by Arizona State University, the University of Arizona, and Western Connecticut State University.

REFERENCES

Ashman, K. M., & Bird, C. M. 1993, AJ, 106, 2281
Aurière, M., Coupinot, G., & Hecquet, J. 1992, A&A, 256, 95
Bajaja, E., & Gergely, T. E. 1977, A&A, 61, 229
Barmby, P., & Huchra, J. P. 2000, ApJ, 531, L29
———. 2001, AJ, 122, 2458
Barmby, P., Huchra, J. P., & Brodie, J. P. 2001, AJ, 121, 1482
Barmby, P., Huchra, J. P., Brodie, J. P., Forbes, D. A., Schroder, L. L., & Grillmair, C. J. 2000, AJ, 119, 727
Battistini, P., Bònoli, F., Braccesi, A., Federici, L., Fusi Pecci F., Marano, B., & Börngen, F. 1987, A&AS, 67, 447
Battistini, P., Bònoli, F., Braccesi, A., Fusi Pecci, F., Malagnini, M. L., & Marano, B. 1980, A&AS, 42, 357
Battistini, P., Bònoli, F., Casavecchia, M., Ciotti, L., Federici, L., & Fusi Pecci, F. 1993, A&A, 272, 77
Borges, A. C., Idiart, T. P., de Freitas Pacheco, J. A., & Thevenin, F. 1995, AJ, 110, 2408
Bressan, A., Chiosi, C., & Tantalo, R. 1996, A&A, 311, 425
Bruzual A., G., & Charlot, S. 1993, ApJ, 405, 538
Buzzoni, A. 1997, in IAU Symp. 183, Cosmological Parameters and Evolution of the Universe, ed. K. Sato (Dordrecht: Kluwer), 134
Calzetti, D. 1997, AJ, 113, 162
Chandar, R., Bianchi, L., & Ford, H. C. 1999a, ApJS, 122, 431
———. 1999b, ApJ, 517, 668
———. 2001, A&A, 366, 498
Charlot, S., & Bruzual A., G. 1991, ApJ, 367, 126
Chiosi, C., Bressan, A., Portinari, L., & Tantalo, R. 1998, A&A, 339, 355
Crampton, D., Cowley, A. P., Schade, D., & Chayer, P. 1985, ApJ, 288, 494
de Freitas Pacheco, J. A. 1997, A&A, 319, 394
Fan, X., et al. 1996, AJ, 112, 628
Fioc, M., & Rocca-Volmerange, B. 1997, A&A, 326, 950
Forbes, D. A., Brodie, J. P., & Grillmair, C. J. 1997, AJ, 113, 1652
Frogel, J. A., Persson, S. E., & Cohen, J. G. 1980, ApJ, 240, 785
Fusi Pecci, F., Cacciari, C., Federici, L., & Pasquali, A. 1993, in ASP Conf. Ser. 48, The Globular Cluster–Galaxy Connection, ed. G. H. Smith & J. P. Brodie (San Francisco: ASP), 410
Galadí-Enríquez, D., Trullols, E., & Jordi, C. 2000, A&AS, 146, 169
Harris, W. E. 1991, ARA&A, 29, 543
Hartwick, F. D. A. 1968, ApJ, 154, 475
Hiltner, W. A. 1958, ApJ, 128, 9
———. 1960, ApJ, 131, 163
Holland, S. 1998, AJ, 115, 1916
Hubble, E. 1932, ApJ, 76, 44
Iye, M., & Richter, O.-G. 1985, A&A, 144, 471
Jablonka, P., Alloin, D., & Bica, E. 1992, A&A, 260, 97
Jablonka, P., Bica, E., Pelat, D., & Alloin, D. 1996, A&A, 307, 385
Kong, X., et al. 2000, AJ, 119, 2745
Kron, G. E., & Mayall, N. U. 1960, AJ, 65, 581
Landolt, A. U. 1983, AJ, 88, 439
———. 1992, AJ, 104, 340
Leitherer, C., et al. 1996, PASP, 108, 996
———. 1999, ApJS, 123, 3
Ma, J., Zhou, X., Chen, J., Wu, H., Jiang, Z., Xue, S., & Zhu, J. 2002a, A&A, 385, 404
———. 2002b, AJ, 123, 3141
Ma, J., Zhou, X., Kong, X., Wu, H., Chen, J., Jiang, Z., Zhu, J., & Xue, S. 2001, AJ, 122, 1796
Mayall, N. U., & Eggen, O. J. 1953, PASP, 65, 24
McClure, R. D., & Racine, R. 1969, AJ, 74, 1000
Mochejska, B. J., Kaluzny, J., Krockenberger, M., Sasselov, D. D., & Stanek, K. Z. 1998, Acta Astron., 48, 455
Mollà, M., Ferrini, F., & Diaz, A. I. 1997, ApJ, 475, 519
Origlia, L., Goldader, J. D., Leitherer, C. Schaerer, D., & Oliva, E. 1999, ApJ, 514, 96
Perrett, K. M., Bridges, T. J., Hanes, D. A., Irwin, M. J., Brodie, J. P., Carter, D., Huchra, J. P., & Watson, F. G. 2002, AJ, 123, 2490
Racine, R. 1991, AJ, 101, 865
Reed, L. G., Harris, G. L. H., & Harris, W. E. 1992, AJ, 103, 824
Rich, R. M., Corsi, C. E., Bellazzini, M., Federici, L., Cacciari, C., & Fusi Pecci, F. 2001, in IAU Symp. 207, Extragalactic Star Clusters, ed. E. K. Grebel, D. Geisler, D. Minniti, in press
Salpeter, E. E. 1955, ApJ, 121, 161
Sargent, W. L. W., Kowal, C. T., Hartwick, F. D. A., & van den Bergh, S. 1977, AJ, 82, 947
Schaerer, D., & de Koter, A. 1997, A&A, 322, 598
Schaerer, D., & Vacca, W. D. 1998, ApJ, 497, 618
Searle, L., Sargent, W. L. W., & Bagnuolo, W. G. 1973, ApJ, 179, 427
Seyfert, C. K., & Nassau, J. J. 1945, ApJ, 102, 377
Stanek, K. Z., & Garnavich, P. M. 1998, ApJ, 503, L131
Stetson, P. B. 1987, PASP, 99, 191
———. 1990, PASP, 102, 932
Tinsley, B. M. 1972, A&A, 20, 383
van den Bergh, S. 1969, ApJS, 19, 145
Vazdekis, A., Peletier, R. F., Beckman, J. E., & Casuso, E. 1997, ApJS, 111, 203
Vetešník, M. 1962a, Bull. Astron. Inst. Czechoslovakia, 13, 180
———. 1962b, Bull. Astron. Inst. Czechoslovakia, 13, 218
Williams, B. F., & Hodge, P. W. 2001, ApJ, 559, 851
Yan, H,. et al. 2000, PASP, 112, 691
Zheng, Z., et al. 1999, AJ, 117, 2757
Zhou, X., Jiang, Z.-J., Xue, S.-J., Wu, H., Ma, J., & Chen, J.-S. 2001, Chinese Astron. Astrophys., 1, 372
Zhou, X., et al. 2002, A&A, in press
Zombeck, M. V. 1990, Handbook of Space Astronomy and Astrophysics (2d. ed; Cambridge: Cambridge Univ. Press), 104